The hnRNP RALY regulates transcription and cell proliferation by modulating the expression of specific factors including the proliferation marker E2F1

Received for publication, May 11, 2017, and in revised form, September 18, 2017 Published, Papers in Press, September 27, 2017, DOI 10.1074/jbc.M117.795591

Nicola Cornella[‡], Toma Tebaldi[§], Lisa Gasperini[‡], Jarnail Singh[¶], Richard A. Padgett[‖], Annalisa Rossi[‡1], and Paolo Macchi[‡2]

From the [‡]Laboratory of Molecular and Cellular Neurobiology, Centre for Integrative Biology, University of Trento, via Sommarive 9, 38123 Trento, Italy, the [§]Laboratory of Translational Genomics, Centre for Integrative Biology, University of Trento, via Sommarive 9, 38123 Trento, Italy, the [‖]Lerner Research Institute, Cleveland, Ohio 44195, and [¶]Deciphera Pharmaceuticals, Lawrence, Kansas 66044

Edited by Joel Gottesfeld

The heterogeneous nuclear ribonucleoproteins (hnRNP) form a large family of RNA-binding proteins that exert numerous functions in RNA metabolism. RALY is a member of the hnRNP family that binds poly-U–rich elements within several RNAs and regulates the expression of specific transcripts. RALY is up-regulated in different types of cancer, and its down-regulation impairs cell cycle progression. However, the RALY's role in regulating RNA levels remains elusive. Here, we show that numerous genes coding for factors involved in transcription and cell cycle regulation exhibit an altered expression in RALY–down-regulated HeLa cells, consequently causing impairments in transcription, cell proliferation, and cell cycle progression. Interestingly, by comparing the list of RALY targets with the list of genes affected by RALY down-regulation, we found an enrichment of RALY mRNA targets in the down-regulated genes upon RALY silencing. The affected genes include the E2F transcription factor family. Given its role as proliferation-promoting transcription factor, we focused on E2F1. We demonstrate that *E2F1* mRNA stability and E2F1 protein levels are reduced in cells lacking RALY expression. Finally, we also show that RALY interacts with transcriptionally active chromatin in both an RNA-dependent and -independent manner and that this association is abolished in the absence of active transcription. Taken together, our results highlight the importance of RALY as an indirect regulator of transcription and cell cycle progression through the regulation of specific mRNA targets, thus strengthening the possibility of a direct gene expression regulation exerted by RALY.

The transcription of DNA into RNA mediated by RNA polymerase II (RNAPII)[3] is a complex process that involves numerous factors, which co-operate with the transcriptional machinery and interact with newly synthesized RNA to ensure its correct processing (1–4). In this context, RNA–binding proteins (RBPs) exert a broad range of functions from the early steps of RNA synthesis until its maturation. For example, they can participate in gene expression regulation by binding chromatin components and interact with nascent RNAs, promoting post-transcriptional modifications, including splicing, nuclear-cytoplasmic shuttling, and RNA transport and stability (5–13). By affecting one or more of these processes, a dysregulation of RBPs might alter the correct expression of fundamental proteins, leading to pathological conditions (14–18). Thus, the tight regulation of transcription and post-transcriptional processing of RNA exerted by RBPs is required for the upstream maintenance of cellular physiology and for the regulation of different processes, including transcription and cell proliferation, which are closely associated. Rapidly proliferating cells show high levels of transcription to sustain the intense demand of gene products necessary to maintain quick growth rates. To this aim, these cells tend to overexpress versatile transcription factors, such as members of the MYC and E2F family, which supply the necessary gene products to promote their growth and division (19).

Among the RBPs involved in the transcriptional regulation and post-transcriptional modification of RNAs, the heterogeneous nuclear ribonucleoproteins (hnRNPs) form a large family of RBPs possessing a broad range of functions in the metabolism of RNA (20–23). Several members of the hnRNP family have been described as interacting with chromatin, DNA, and RNA to influence transcription and RNA processing (24). For example, the hnRNPs C1/C2 interact with newly synthesized transcripts through their RNA-binding domain, regulating RNA stability and RNA nuclear export (12, 25, 26). hnRNP-U, which binds chromatin and is involved in pre-mRNA processing, also regulates RNAPII transcription by binding to its

This work was supported by the University of Trento (Progetto Biotecnologie) and the Autonomous Province of Trento (MaDEleNA Project) (to P. M.). The authors declare that they have no conflicts of interest with the contents of this article.

This article contains supplemental Figs. S1–S4 and Tables S1–S3.

[1] To whom correspondence may be addressed. Tel.: 39-0461-283819; Fax: 39-0461-283937; E-mail: annalisa.rossi-1@unitn.it.

[2] To whom correspondence may be addressed. Tel.: 39-0461-283819; Fax: 39-0461-283937; E-mail: paolo.macchi@unitn.it.

[3] The abbreviations used are: RNAPII, RNA polymerase II; RBP, RNA–binding protein; RNP, ribonucleoprotein; hnRNP, heterogeneous nuclear ribonucleoprotein; qRT-PCR, quantitative real-time PCR; GSEA, gene set enrichment analysis; RIP, RNA immunoprecipitation; ActD, actinomycin D; 5-EU, 5-ethynyl uridine; Rb, retinoblastoma; ncRNA, noncoding RNA; NSB, nucleus separation buffer; DEG, differentially expressed genes; FDR, false discovery rate; MSigDB, Molecular Signatures Database; 5-FAM, 5-carboxyfluorescein; 5,6-dichloro-l-D-ribofuranosylbenzimidazole.

C-terminal domain or to the preinitiation complex (27, 28). Moreover, hnRNP-K exerts a transcriptional control activity by interacting with DNA on regulatory elements upstream of the promoters but also by binding specific RNAs to recruit the termination factor XRN2 (24, 29).

RALY is a member of the hnRNP family that was initially identified as a cross-reacting autoantigen with the Epstein-Barr nuclear antigen 1 (EBNA1), a viral protein encoded by the Epstein-Barr virus (30). RALY contains an RNA-recognition motif (RRM) at the N terminus, two predicted nuclear localization signals, and a glycine-rich region at the C terminus (25, 31). We recently identified RALY RNA targets by performing RIP-seq analysis in MCF7 cells and studied the gene expression profile of RALY-silenced MCF7 cells. The two analyses identified 2929 RNAs bound by RALY and 217 differently expressed genes consequent to its down-regulation (32). Crossing these results, we selected 23 genes that are differently expressed after RALY silencing and for which the transcript is bound by RALY. Among these targets, we focused on *ANXA1* and *H1FX*, which were found, respectively, to be up- and down-regulated both at the RNA and the protein level upon RALY silencing. We also characterized the RNA-binding property of RALY by showing that it binds poly-U stretches, preferentially positioned in the 3′-UTR of protein-coding transcripts (32). Through proteomic analysis, RALY was found to interact with the C-terminal domain of RNAPII as well as with proteins involved in RNA metabolism and translational control, including polysomes (31–33).

In a recent study, RALY was found to interact with the long-noncoding RNA *LeXis* and with promoters of genes involved in the cholesterol biosynthesis pathway in mouse liver (34). An increased expression of *LeXis* determined a decrease in the cholesterol content of mice blood serum. Interestingly, when *LeXis* was up-regulated, Sallam *et al.* (34) detected a lesser presence of RALY on the promoters of genes involved in cholesterol biosynthesis, with a consequent reduced expression of their mRNA. The same phenotype was observed when RALY was down-regulated with *LeXis* in a wild-type condition, and no effects of *LeXis* expression were observed in RALY-defective mice. These results, which highlight a transcriptional regulatory activity of RALY, although not in detail, induced Sallam *et al.* (34) to propose RALY as a transcriptional co-factor. Altogether, these data suggest that RALY plays differing roles in the processing and post-transcriptional modification of RNA.

Here, we studied the gene expression profile of HeLa cells in response to RALY silencing to better characterize the impairment in cell cycle progression observed previously by Rossi *et al.* (32). We found that mRNAs coding for several factors involved in the regulation of cell proliferation and transcription were down-regulated upon RALY silencing. In particular, we focused on the interaction between RALY and *E2F1* mRNA, a well-characterized marker of cell proliferation and regulator of the cell cycle (35). We demonstrated that RALY regulates the expression and the stability of *E2F1* mRNA and therefore the amount of E2F1 protein inside the cells. In agreement with our findings, the deletion of RALY in HeLa cells caused a reduction of cell proliferation and a stall in the G_1 phase of the cell cycle. Moreover, RALY silencing caused a global reduction of RNAPII-dependent transcription. To understand in more detail the role of RALY in gene expression regulation, we then studied the interaction of RALY with chromatin. We show that RALY can interact with transcriptionally active chromatin through two different regions in both an RNA-dependent and -independent manner. Taken together, our results demonstrate that RALY regulates cell proliferation and transcription by modulating the expression of several key factors of the two processes, and add evidence of the direct involvement of RALY to gene expression regulation by characterizing its binding to transcriptionally active chromatin.

Results

The down-regulation of RALY impairs the expression of cell cycle– and transcription–related genes

We recently observed that the silencing of RALY in MCF7 cells caused the down-regulation of different genes related to cell cycle progression and that RALY–down-regulated cells showed a reduction in cell growth rate compared with control cells (32). Furthermore, transcripts coding for cell cycle–related proteins were enriched among the RNA bound by RALY (32). To characterize the role of RALY in cell proliferation, we studied the gene expression profile of HeLa cells after RALY down-regulation. We used a HTA2.0 microarray (Affymetrix Human Transcriptome Array) to analyze three different biological replicas of HeLa cells transfected with either siRNA against RALY (si-RALY) or control siRNA (si-CTRL) for 72 h. The levels of *RALY* mRNA measured by quantitative real-time PCR (qRT-PCR) were detected at levels below 10% in si-RALY–transfected cells compared with control cells (Fig. 1*A*).

After RALY silencing, we found 1971 differentially expressed genes, of which 919 were up-regulated and 1052 down-regulated (Fig. 1*B* and supplemental Table S1). The majority of the variations was observed in protein coding transcripts (93.5%), with a small percentage of noncoding RNAs, generally higher among up-regulated genes (3% of the long noncoding RNA) (Fig. 1*C*). Functional annotation enrichment analysis by gene ontology and pathways databases identified extracellular matrix organization, regulation of cell motility, and cell adhesion as the biological processes that were significantly associated with the up-regulated genes. On the other hand, cell cycle control and RNA splicing were the two broad themes strongly associated with the down-regulated genes upon RALY silencing (Fig. 1*D* and supplemental Table S2). Interestingly, several genes coding for factors involved in transcription regulation were present in the list of down-regulated genes (supplemental Table S1).

To have a more comprehensive understanding of the general function of RALY on its target mRNAs, we intersected the list of differentially expressed genes detected in HeLa cells with the list of RALY targets identified previously by RIP-seq in MCF7 cells (32). We found that 193 up-regulated genes and 359 down-regulated genes were present in both lists (Fig. 1*E*). Although this intersection could be underestimated due to cell line differences, the increased frequency of RALY RNA targets among genes down-regulated upon RALY silencing (34.1 *versus* 21%, p value, 1.3e-10) suggests that the loss of a direct RALY–mRNA interaction might explain the observed down-regulation (Fig. 1*E*).

Taking into account this correlation between gene expression down-regulation and RALY silencing, and considering that cell proliferation and transcription are two closely related processes (19), we focused on the down-regulated genes upon RALY silencing. To validate the down-regulation events detected by microarray, we measured the expression of factors promoting cell proliferation and/or RNA transcription by qRT-PCR. We validated the mRNA expression of different factors involved in cell cycle progression, such as *CCNB1*, *CCNB2*, and *CDK1*, which together drive the G_2/M transition; *CCNE1* and *CCNE2*, two regulators of the entry into S phase, and *CDC25A*, a phosphatase involved in both S-phase entry and the G_2-phase transition (Fig. 2*A*) (36–38). Regarding transcription, we validated the mRNA expression of different transcription-promoting factors such as *CCNT1*, the cyclin subunit of positive transcription elongation factor b (P-TEFb), that is responsible for

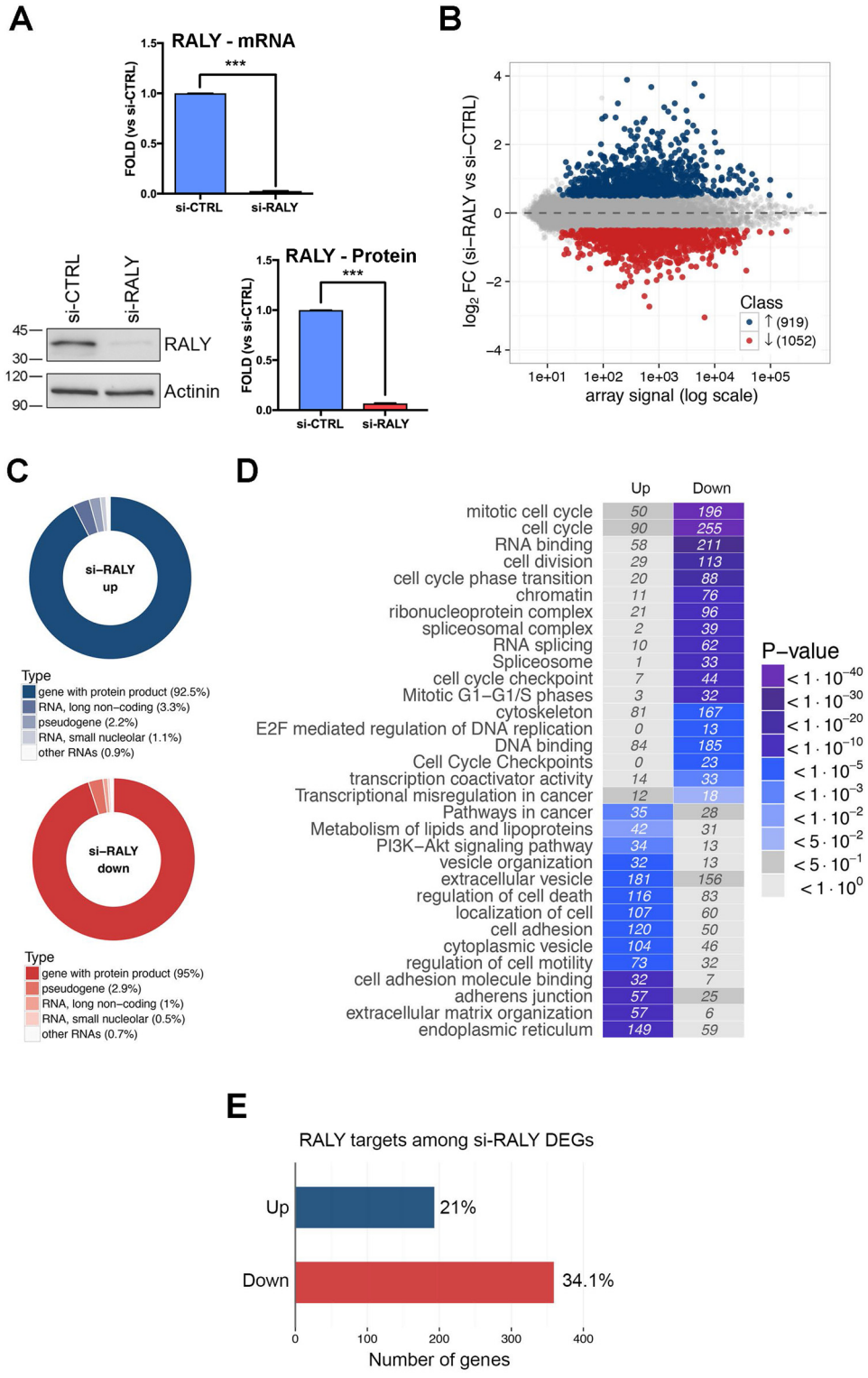

the release of RNAPII from promoter-proximal pausing and for the activation of RNAPII productive elongation; *GTF2A1* and *GTF2E2*, subunits of general transcription factors involved in transcription initiation; and *ELL2*, a member of the transcription-promoting super elongation complex (Fig. 2*A*) (39–42). In addition, the two subunits of the facilitating transcription (FACT) complex, *SUPT16H* and *SSRP1*, were found to be down-regulated at the mRNA level (Fig. 2*A*). The FACT complex has been described as associating with active RNAPII and promoting nucleosome disassembly to facilitate transcription (43–45). All of the target mRNAs were found to be down-regulated in si-RALY–transfected HeLa cells, which confirms the microarray data (Fig. 2*A*). In addition, we measured the protein levels of CCNE1 and CCNT1 by Western blot analysis and found both down-regulated in si-RALY cells (Fig. 2, *B* and *C*).

RALY binds E2F1 mRNA and regulates its stability

To improve the functional characterization of the deregulated transcripts upon RALY silencing, we performed gene set enrichment analysis (GSEA) over the collection of "hallmark" annotated gene sets provided by the Molecular Signatures Database (MSigDB) (46). This analysis identified the targets of the E2F transcription factors family as the class of genes most significantly enriched among the genes down-regulated upon RALY silencing (Fig. 3A). This gene set, according to the MSigDB definition, includes "genes encoding cell cycle related targets of E2F transcription factors."

The E2F family encodes for eight transcription factors that play key roles in the regulation of cell cycle progression. Its members can be divided into activators (E2F1–3) and repressors (E2F4–5, E2F6, and E2F7–8) of cell proliferation (47). In particular, the E2F1–3 group, which regulates the transactivation of genes necessary for the G_1/S-phase transition of the cell cycle, was found to be down-regulated in the microarray data upon RALY silencing (supplemental Table S1). On the contrary, only the repressors E2F7 and E2F8 showed an altered expression in si-RALY–treated cells, being up- and down-regulated, respectively, whereas no variations were found for repressor group E2F4–6 (supplemental Table S1). Interestingly, *E2F1* and *E2F2* mRNAs were identified previously as specific targets of RALY in the RIP-seq experiment performed in MCF7 cells, whereas all the proliferation repressors of the E2F family were not detected as RALY RNA interactors (Fig. 3*B*) (32).

Among the misregulated activators of the E2F family, we focused on E2F1, a key regulator of the cell cycle and apoptosis, also involved in carcinogenesis when misexpressed (19, 48–51). First, we confirmed its down-regulation in RALY silenced cells both at the mRNA and protein level by qRT-PCR and Western blot analyses, respectively (Fig. 3, *C* and *D*). The down-regulation of E2F1 was confirmed also in stable RALY knock-out HeLa cells (RALY KO) generated by CRISPR/Cas9 technology compared with control vector-transfected HeLa cells (PX330) (supplemental Fig. S1 and Fig. 3*E*) (32).

Next, we analyzed whether *E2F1* mRNA was enriched in RALY-containing ribonucleoparticles (RNPs) by performing an RNA immunoprecipitation (RIP) assay after UV cross-linking in HeLa cells followed by qRT-PCR analysis. As expected, *E2F1* transcript was significantly enriched in RALY immunoprecipitates compared with both rabbit IgG and the amount of *GAPDH* mRNA, which was used as a negative control (Fig. 4*A*). *RALY* mRNA was used as a positive control (32).

We recently demonstrated that RALY preferentially interacts with poly-U stretches with four or more uridines within the 3′-UTR of transcripts (32). To confirm the direct interaction and to identify the region bound by RALY on *E2F1* mRNA, we selected a suitable poly-U stretch in the 3′-UTR of *E2F1* mRNA and performed RNA pulldown experiments using either a wild-type or a mutated RNA probe (Fig. 4*B*). As a positive control, we used a probe containing the poly-U stretch of the *H1FX* 3′-UTR (32). RALY was pulled down by the wild-type but not by the mutated probe of *E2F1* 3′-UTR poly-U stretch (Fig. 4*B*). In contrast, neither tubulin nor actinin was detected upon incubation with all the probes, excluding the possibility of unspecific bindings (Fig. 4*B*). As expected, the *H1FX* RNA probe pulled down RALY from the cell lysate (Fig. 4*B*). Taken together, these results show that RALY interacts with *E2F1* mRNA.

Because the 3′-UTRs are often targeted by trans-acting factors to determine the fate of the mRNAs, we decided to investigate whether RALY could regulate *E2F1* mRNA at the post-transcriptional level. In the range of possible post-transcriptional modifications, we analyzed transcript stability, as other members of the hnRNP family, in particular hnRNP-C, which shares a high similarity with RALY in the RRM, are described as regulating the stability of specific transcripts (12, 21, 52–54). HeLa cells were transfected with either si-CTRL or si-RALY for 72 h and then treated with actinomycin D (ActD, 5 μg/ml) for different periods of time to prevent new RNA synthesis. The total RNA was then extracted and analyzed by qRT-PCR. As shown in Fig. 5*A*, the stability of *E2F1* in RALY-silenced HeLa cells was measurably lower over time compared with control cells, with a half-life of 7.64 ± 1.32 h. In contrast, *E2F1* was stable over the 9-h analyzed time-frame in cells trans-

Figure 1. RALY silencing alters the transcriptome of HeLa cells. Three independent microarray experiments were performed using RNA preparations from three independent biological replicates of HeLa cells transfected with either si-RALY or si-CTRL for 72 h. *A*, to assess RALY silencing, total RNA and protein extracts were analyzed through qRT-PCR (normalized on *GAPDH*) and subjected to SDS-PAGE and Western blot analysis, respectively, with the indicated antibodies. The cells analyzed by microarray showed down-regulation of RALY at both the mRNA (*upper graph*) and protein (*lower graph*) levels. The graphs show the mean of three independent experiments ± S.D. The *p* value was calculated using an unpaired two-tailed *t test* (***, $p < 0.001$). *B*, MA plot of RALY-silencing transcriptome profiling. For each gene, the average log10 signal against the RALY-silencing log2 fold change (si-RALY *versus* control) is plotted. Genes significantly up-regulated (*blue*) or down-regulated (*red*) upon RALY silencing are highlighted. *C*, classification of DEGs upon RALY silencing according to RNA classes. *D*, functional annotation enrichment analysis of RALY– up-regulated and –down-regulated genes. The heat map, colored-coded according to enrichment *p* value, displays enriched classes from gene ontology terms and the KEGG or REACTOME pathways. The *number* of DEGs falling in each category is displayed inside each tile. *E*, intersection between the lists of si-RALY up-regulated (*blue*) or down-regulated (*red*) genes in HeLa cells and the list of RALY RIP-seq targets identified previously in MCF7 cells (32). The *percentage* of overlap with respect to the number of DEGs is displayed beside the corresponding *bar*. Although the intersection could be affected by cell line differences, the increased frequency of RALY RNA targets among genes down-regulated upon RALY silencing suggests that the loss of a direct RALY–mRNA interaction is associated with the down-regulation of the target.

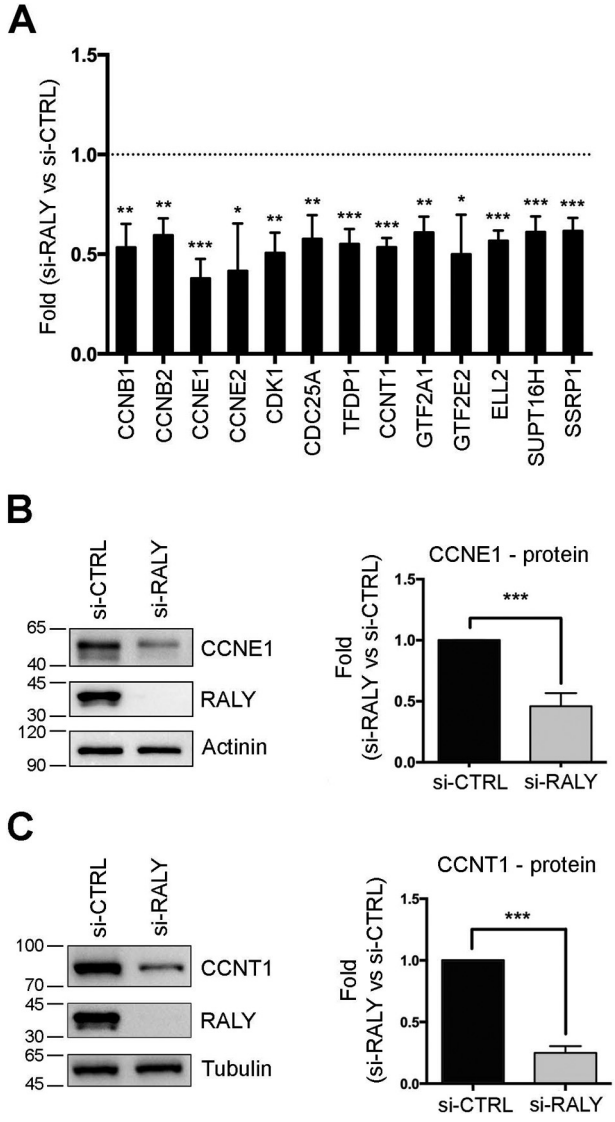

Figure 2. Validation of the microarray results for down-regulated genes upon RALY silencing. *A*, HeLa cells were transfected with either si-RALY or si-CTRL for 72 h, and total RNA was extracted. The mRNA levels of the different factors promoting proliferation (*CCNB1*, *CCNB2*, *CCNE1*, *CCNE2*, *CDK1*, *CDC25A*, and *TFDP1*) and transcription (*CCNT1*, *GTF2A1*, *GTF2E2*, *ELL2*, *SUPT16H*, and *SSRP1*) were measured by qRT-PCR and normalized on *GAPDH*. As in the microarray analysis, all of the analyzed genes were found to be less expressed in si-RALY cells compared with si-CTRL cells. *B* and *C*, total protein extracts were produced from HeLa cells transfected with either si-RALY or si-CTRL for 72 h. Total lysates were subjected to SDS-PAGE, and Western blot analysis with the indicated antibodies (*left panels*). The levels of CCNE1 (*B*) and CCNT1 (*C*) were analyzed by band densitometry analysis (*right panels*) and found to be down-regulated in si-RALY– compared with si-CTRL–transfected cells. All of the graphs show the mean of three independent experiments ± S.D. The *p* value was calculated using an unpaired two-tailed *t test* (*, $p < 0.05$; **, $p < 0.01$; ***, $p < 0.001$) between the signal detected in si-RALY– and si-CTRL–transfected cells.

fected with si-CTRL. As a control, we used the mRNA coding for *GAPDH*, a non-target of RALY (Fig. 4*A*) considered a suitable control for assessing general mRNA stability (55). *GAPDH* mRNA was found to be stable over 9 h in both si-CTRL and si-RALY–transfected cells (Fig. 5*B*).

Taken together, these results show that the silencing of RALY induces a broad down-regulation of cell cycle– and transcription–related genes. Moreover, we show that RALY binds *E2F1* mRNA and that in its absence, the stability of *E2F1* mRNA is reduced. Consequently, both E2F1 mRNA and protein are down-regulated in RALY-silenced cells. Interestingly, cells expressing high levels of endogenous RALY, such as the cancerous cell lines Panc-1 and MDA-MB-231, also showed a higher expression of E2F1, compared with the less aggressive HPNE and MCF7 cell lines (Fig. 5*C*).

The silencing of RALY affects cell cycle progression

To understand whether these down-regulated genes could induce specific effects in HeLa cells, we measured cell proliferation, cell cycle distribution, and global RNA transcription of RALY KO and RALY-silenced HeLa cells. Cell proliferation was measured through the real-time cell analysis platform, xCELLigence (56, 57). The proliferation rate of RALY KO cells was reduced compared with control cells (PX330) (Fig. 6*A*). To analyze the cell cycle distribution, we sorted the cells into the different phases of the cell cycle by measuring their DNA content through the incorporation of the thymidine analogue 5-ethynyl-deoxiuridine into newly synthesized DNA, successive staining with 5-FAM, and analysis with the high-content imaging system Operetta™ (58). In accordance with our previous results, RALY KO cells showed a significant enrichment in the G_1 phase and a consequent lower number of cells in S phase compared with control cells (Fig. 6*B*). For both experiments, similar results were obtained for RNAi-RALY– down-regulated cells (supplemental Fig. S2). These results show that the down-regulation of RALY affects the normal progression of the cell cycle and impairs cell proliferation.

The silencing of RALY affects RNA transcription

To evaluate any general effect of RALY silencing on RNA transcription, we transfected HeLa cells with either si-RALY or si-CTRL for 72 h and measured the nuclear levels of newly synthesized RNA over different periods of time through the incorporation of 5-ethynyl uridine (5-EU) into new transcripts and successive staining with the fluorescent molecule 5-FAM using a click reaction (59). The down-regulation of RALY was verified and quantified by immunostaining using the high-content imaging system (Fig. 7*A*). Notably, for the quantification of newly synthesized RNA we selected only the successfully RALY– down-regulated cells by setting a threshold on the RALY fluorescence signal. As expected, the levels of newly synthesized RNA showed a slower increase over time in cells lacking RALY compared with control cells (Fig. 7*B*).

Because ribosomal RNAs are the most abundant and actively transcribed RNA species inside cells, RNA staining yielded an intense fluorescent signal in the nucleoli, making the differences in the nuclear RNA levels difficult to measure accurately. To overcome this problem, and given the fact that RALY is not present inside the nucleoli, we treated the cells with a low dose of ActD (125 ng/ml) to specifically block the activity of RNA polymerase I (59). Following this treatment, the nucleolar RNA signal was reduced (Fig. 7*C*). The down-regulation of RALY was verified by immunofluorescence (Fig. 7*D*). Under these conditions, si-RALY–transfected cells showed a slower increase over time of nuclear newly synthesized RNA compared with si-CTRL transfected cells (Fig. 7*E*).

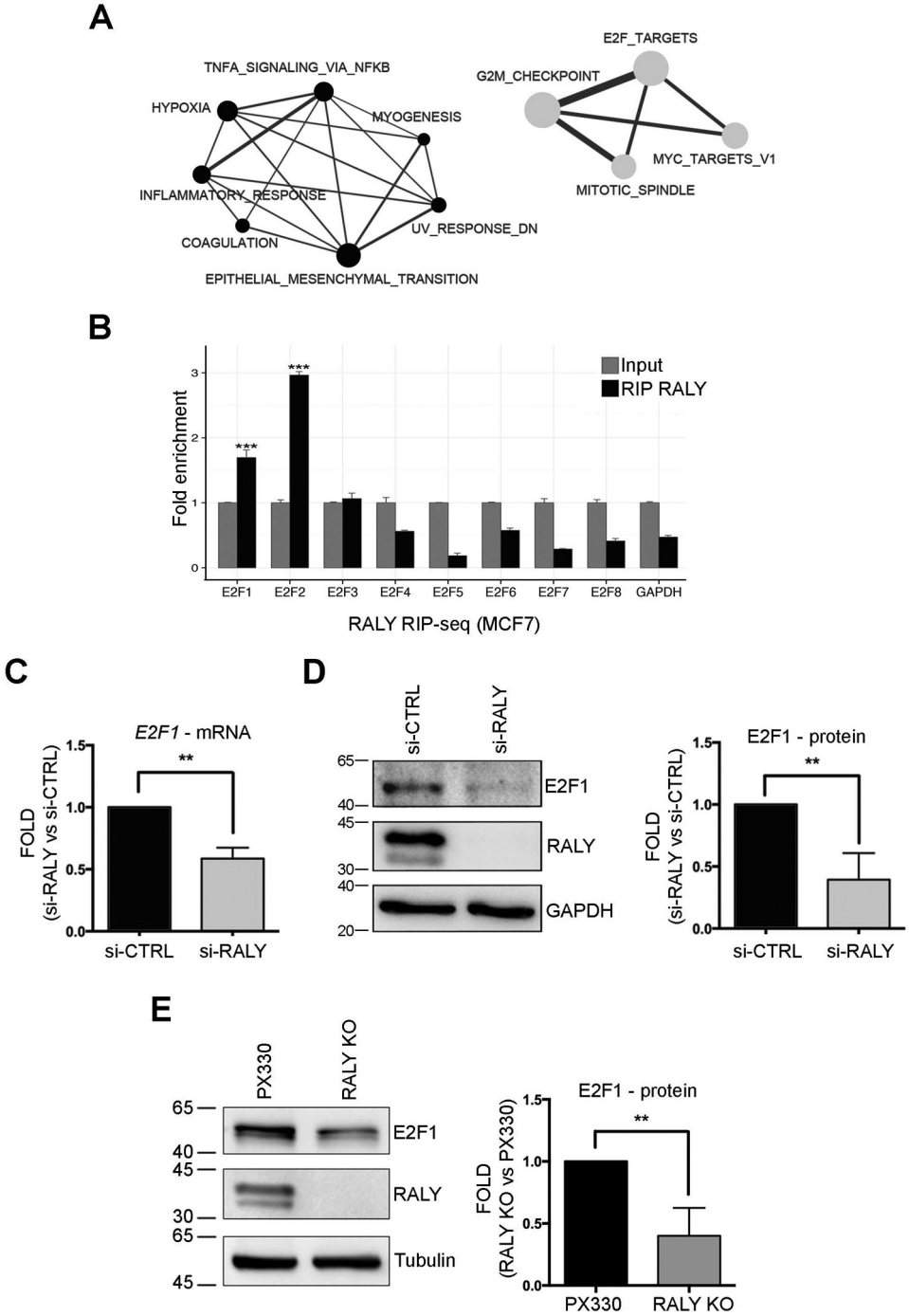

Figure 3. RALY regulates E2F1 expression. *A*, functional map of global changes in gene expression in response to RALY silencing. Enrichment results from GSEA were mapped as a network of gene sets (nodes) related by mutual overlap (edges), where *black* identifies the up-regulated and *light gray* the down-regulated gene sets. The size of each node is proportional to the size of the gene set. The size of each edge is proportional to the mutual overlap between two nodes. The gene set *E2F_TARGETS*, which contains "genes encoding cell cycle–related targets of E2F transcription factor," is the most enriched in down-regulated genes upon RALY silencing. *B*, the mRNAs coding for *E2F1* and *E2F2* were found to be enriched in RALY-containing immunoprecipitated particles in the RIP-seq analysis performed in MCF7 cells. On the contrary, no enrichment was detected for the other members of the E2F family. The graphs represent the mean of three independent experiments ± S.D. The *p* value was calculated using an unpaired two-tailed *t* test between the respective samples (***, $p < 0.001$). *C* and *D*, HeLa cells were transfected with either si-RALY or si-CTRL for 72 h, and both total RNA and total protein extracts were collected. RNA was analyzed by qRT-PCR and the signals normalized on *GAPDH*, whereas proteins were subjected to SDS-PAGE and Western blot analysis with the indicated antibodies followed by band densitometry analysis. Both the *E2F1* mRNA (*C*) and E2F1 protein (*D*) are down-regulated in cells lacking RALY expression. *E*, PX330 and RALY KO lysates were subjected to SDS-PAGE and Western blot analysis using the indicated antibodies followed by band densitometry analysis. E2F1 expression is reduced in RALY KO cells. The *graphs* show the mean of three independent experiments ± S.D. The *p* value was calculated using an unpaired two-tailed *t* test (**, $p < 0.01$).

To confirm that the effect on general transcription was specifically caused by RALY down-regulation, we also measured RNA synthesis in RALY KO cells. As for the RNAi experiments, RALY KO cells showed a decreased synthesis of RNA compared with PX330 cells (supplemental Fig. S3*A*). The decrease in RNA synthesis was also observed in RALY KO cells upon RNA poly-

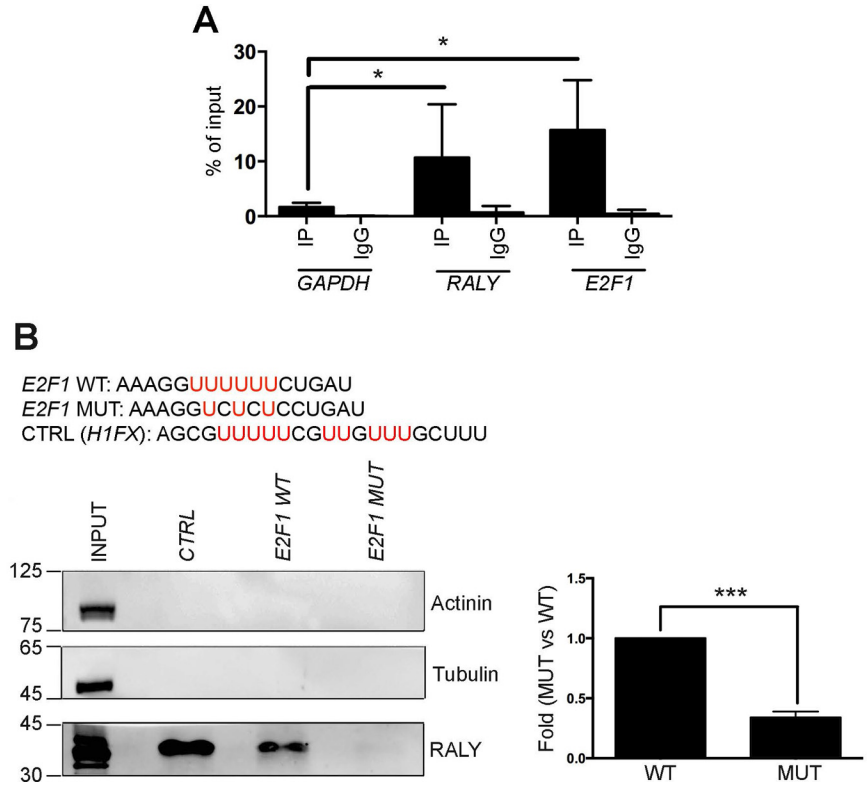

Figure 4. RALY interacts with *E2F1* mRNA *A*, qRT-PCR was used to compare the indicated mRNAs isolated upon UV–cross-linked RALY immunoprecipitation. RNA was recovered after immunoprecipitation with anti-RALY and control anti-IgG antibodies. The relative abundance was compared with 10% of input. *E2F1* mRNA is enriched in RALY-containing RNPs. *Bars* represent means ± S.D. of three independent experiments. The *p* value was calculated by comparing the amount of each mRNA with the amount of *GAPDH* using an unpaired two-tailed *t* test (*, $p < 0.05$). *B*, sequences of the biotinylated wild-type and mutant E2F1 3′-UTR probes (*top*). Total protein extract from HeLa cells was incubated with either E2F1 wild-type (*WT*) or mutant (*MUT*) biotinylated RNA probes (50 pmol) and captured by streptavidin–Dynabeads. *H1X* 3′-UTR biotinylated probe was used as a positive control (*CTRL*) as described by Rossi *et al.* (32). Western blot analysis of probe-bound proteins showed the positive *in vitro* interaction of RALY with the wild-type poly-U sequence but not with the mutant probe. Immunoblotting with anti-actinin and anti-tubulin served as negative controls. The *graph* shows the mean values of the densitometry analysis of three independent experiments. *Bars* represent mean ± S.D. The *p* value was calculated by an unpaired two-tailed *t* test (***, $p < 0.001$).

merase I block, confirming that the effect observed with RNAi was specifically related to RALY down-regulation (supplemental Fig. S3*B*). These results show that in absence of RALY, the synthesis of new RNA by RNAPII is significantly decreased.

The absence of RALY does not impair RNAPII elongation

To determine whether the reduction in RNA synthesis could be the result of a slower RNAPII–RNA polymerization, we measured the rate of RNAPII elongation (60). We blocked RNAPII-dependent transcription by treating the cells with DRB (100 μM) for 3 h. During this time, any pre-mRNAs could be processed but no new RNA was transcribed. The cells were washed extensively with PBS and incubated with new media to recover transcription, and total RNA was extracted at 5-min intervals until 120 min of reactivation was reached. qRT-PCR was performed with different exon-intron–spanning primers to measure the RNAPII elongation rate (60).

We measured the elongation speed of RNAPII on three genes: *ITPR1*, where the level did not change upon RALY down-regulation; and *OPA1* and *CTNNBL1*, which were, respectively, up-regulated and down-regulated in cells in which RALY was silenced (Fig. 8*A*). These genes were selected based on length, so that RNAPII transcription could be appreciably measured at 5-min intervals by qRT-PCR. For all of the analyzed genes, the elongation speed in cells lacking RALY was comparable with that of the control cells (Fig. 8, *B–E*). However, the amount of synthesized pre-mRNA was lower in cells where RALY was down-regulated, suggesting that a lower number of transcriptional events had taken place compared with control cells (Fig. 8, *B–D*). Taken together, these results show that the down-regulation of RALY affected RNAPII-dependent transcription by lowering the total amount of newly synthesized RNA without affecting RNAPII dynamics.

RALY associates with chromatin in both an RNA-dependent and -independent manner

Our results showed the involvement of RALY in the regulation of cell proliferation and transcription. We demonstrated that RALY controlled the expression of the proliferation marker E2F1 at the post-transcriptional level, thus regulating its stability. However, RNA-binding proteins may have a plethora of roles both in the biogenesis and post-transcriptional modifications of RNA. Regarding this possibility, RALY was recently described as a transcriptional co-factor (34). For these reasons and to better define a possible direct role of RALY in the regulation of gene expression, we decided to study the interaction of RALY with chromatin more in details.

As reported previously, RALY interacts with proteins that have the ability to bind chromatin to exert different functions related to gene expression and transcriptional control (13, 24,

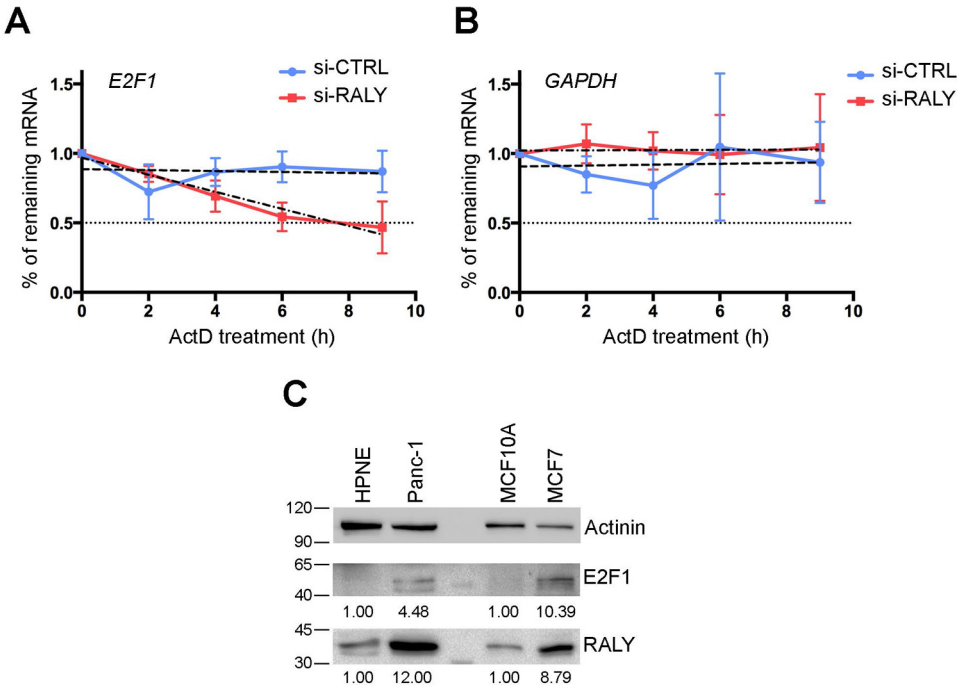

Figure 5. RALY stabilizes *E2F1* mRNA. *A* and *B*, HeLa cells were transfected either with si-RALY or si-CTRL for 72 h and treated successively with ActD (5 μg/ml) for 0, 2, 4, 6, and 9 h. Total RNA was extracted and analyzed through qRT-PCR and normalized on the *ACTB* signal. *A*, *E2F1* mRNA is less stable in si-RALY–transfected cells compared with control untreated cells. *E2F1* mRNA was measured to have a half-life of 7.64 $\pm$ 1.32 h in si-RALY cells but remained stable for over 9 h in si-CTRL cells. *B*, on the contrary, *GAPDH* mRNA is comparably stable in both si-RALY– and si-CTRL–transfected cells. *C*, HPNE, Panc-1, MCF10A, and MCF7 cells were lysed, and the total protein extracts were subjected to SDS-PAGE and Western blot with the indicated antibodies. Bands were quantified through band densitometry analysis and normalized on actinin. The more aggressive cell lines, Panc-1 and MCF7, express higher levels of both RALY and E2F1 compared with the less aggressive cell lines, HPNE and MCF10A, highlighting the positive relationship between RALY and E2F1 expression.

31). We fractionated HeLa cells into four different fractions: cytosolic, nuclear-soluble, and low-salt– and high-salt–soluble chromatin fractions (13, 61). The cytosolic fraction contains all of the extranuclear proteins, whereas the nuclear-soluble fraction comprises the nuclear proteins not attached to chromatin. The low-salt–soluble chromatin fraction contains proteins associated with transcriptionally active chromatin and with transcription start sites. Finally, the high-salt–soluble chromatin fraction contains proteins associated with transcriptionally inactive chromatin and bulky complexes strongly associated with chromatin (13, 61). The enrichment of RALY in these different fractions was analyzed using Western blot analysis.

To verify the success of the fractionation, we used β-tubulin, linker histone H1X, and histone H3 as the cytosolic, inactive chromatin, and whole chromatin markers, respectively. As expected, H1X was found in the high-salt–soluble fraction but not in the low-salt–soluble fraction of chromatin (Fig. 9*A*, *lanes LS* and *HS*). In contrast, H3 was present in both chromatin fractions (Fig. 9*A*). β-Tubulin instead was enriched exclusively in the cytosolic fraction (Fig. 9*A*, *lane C*). When we analyzed the distribution of RALY, we found that an equal amount was present in the fractions containing transcriptionally active and inactive chromatin-bound proteins (Fig. 9*A*). Moreover, RALY was also present in the nuclear-soluble fraction. Finally, we compared RALY distribution with FUS/TLS, a well-characterized member of the hnRNPs (62–66). RALY and FUS showed a similar association with the nuclear-soluble and transcriptionally active chromatin fractions but had a different interaction with the high-salt–soluble chromatin (Fig. 9*A*). The association of FUS with chromatin has been described as strictly RNA-dependent (13), whereas a portion of RALY persists on chromatin even in the absence of RNA, suggesting different molecular functions of the two RBPs. However, considering that FUS has been identified as an interactor with RALY through mass spectrometry and that RALY is characterized as a transcriptional co-factor (31, 34), this shared association opens the interesting possibility of a co-operative function for the two hnRNPs in transcriptional control and RNA maturation.

To assess the involvement of RNA in the RALY–chromatin interaction, we treated cell pellets with RNase A prior to the fractionation process (Fig. 9*B*). Upon RNase A treatment, a statistically significant amount of RALY shifted from the low-salt–soluble chromatin fraction to the cytosolic fraction (Fig. 9, *B*, *lanes 1* and *2* and *5* and *6*, and *C*). Interestingly, the fraction of RALY associated with transcriptionally inactive chromatin did not shift upon RNA degradation (Fig. 9*B*, *lanes 7* and *8*). Taken together, these results demonstrate for the first time that RALY binds both transcriptionally active and inactive chromatin. Moreover, our data show that the interaction of RALY with active chromatin is only partially dependent on RNA.

To identify the regions of RALY involved in the interaction with chromatin, we produced constructs coding for different domains of RALY predicted previously by computational analysis (31). The constructs were tagged with a c-Myc tag at the C terminus and encompassed the N-terminal region (amino acids 1–225), the C-terminal region (amino acids 143–306), and the unstructured glycine-rich region (amino acids 225–306) (Fig. 10*A*). A c-Myc–tagged full-length RALY (*FL*, amino acids 1–306) (Fig. 10*A*) and the empty expression vector were used as positive and negative controls, respectively. The expression of

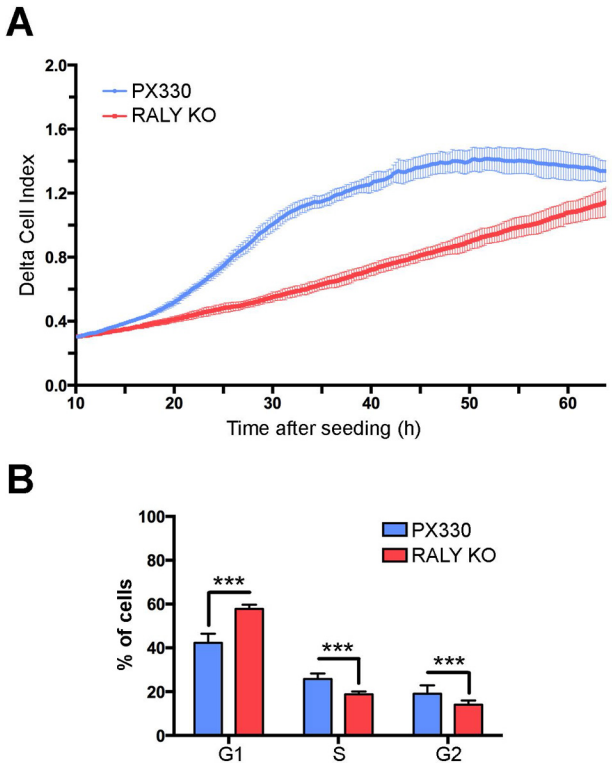

Figure 6. The absence of RALY impairs cell proliferation and cell cycle progression. *A*, PX330 and RALY KO cells were plated into an xCELLigence RTCA (real-time cell analyzer) E-plate, and cell proliferation was monitored for 60 h. RALY KO cells show a decreased cell proliferation compared with PX330 control cells. *B*, PX330 and RALY KO cells were seeded into a 96-well plate and left to grow for 24 h. The cells were then incubated with 10 μM 5-EdU for 1 h and processed to stain newly synthesized DNA. The cells were analyzed using a high-content imaging system, and the distribution of the cells through the cell cycle was evaluated depending on their DNA content. RALY KO cells show an enrichment in the G_1 phase of the cell cycle and a consequent lower distribution in both the S and G_2 phases. The *graphs* show the mean values of three independent experiments. *Bars* represent mean ± S.D. The *p* value was calculated by unpaired two-tailed *t* test (**, $p < 0.01$; ***, $p < 0.001$).

each construct in HeLa cells was analyzed by Western blot analysis (Fig. 10*B*).

We analyzed the subcellular localization of the recombinant proteins by fluorescence microscopy. All RALY fragments localized into the nucleus, with the exception of region 143–306, which also showed a signal in the cytoplasm (Fig. 10*C*). Then, we assessed the distribution of each fragment upon cell fractionation. Although all constructs were enriched in the nuclear fractions, their distribution changed upon RNase A treatment (Fig. 10*D*). In the absence of RNA, the N-terminal part of RALY containing the RRM (amino acids 1–225) disappeared from the nuclear-soluble and low-salt–soluble chromatin fractions (Fig. 10*D*, *NS* and *LS*). This behavior was not observed for the C-terminal part (amino acids 143–306) (Fig. 10*D*, *NS* and *LS*). As expected, full-length RALY decreased in the low-salt–soluble chromatin fraction after RNase A treatment but not in the high-salt–soluble chromatin fraction, confirming that RALY–Myc behaved the same as endogenous RALY (Fig. 10*D*, *LS* and *HS*).

These results underline the importance of RNA in the interaction of RALY with transcriptionally active chromatin and show that RALY can interact with chromatin using either the N- or C-terminal region. However, only the binding with transcriptionally active chromatin, which involves the N-terminal RRM domain, is dependent on the presence of RNA.

The localization of RALY is dependent on active transcription

Because the activity and localization of RBPs is directly related to RNA, we focused on the RNA-dependence quality of RALY interaction with transcriptionally active chromatin. We asked whether RALY localization and its association with chromatin could be affected by the inhibition of transcription. Therefore, we blocked transcription with ActD (5 μg/ml) for different periods of time and analyzed the intracellular localization of RALY with a high-content imaging system (Operetta™). The inhibition of transcription was verified by measuring the newly synthesized RNA through the incorporation of 5-EU into new transcripts and successive staining with 5-FAM using Click-iT reaction (59). As expected, no incorporation of 5-EU was detected in HeLa cells treated with ActD (Fig. 11, *A* and *B*).

Interestingly, RALY nuclear staining decreased over time, suggesting that the ActD treatment activated either RALY degradation or translocation from the nucleus to the cytoplasm (Fig. 11, *A* and *C*). Because the increase in the RALY signal in the cytoplasm was close to the sensitivity limit of the high-throughput microscope for reliable quantification, we analyzed the localization of RALY by cell fraction after treating the cells with either ActD or DMSO (as control). After treating the cells with ActD, the level of RALY in the low-salt–soluble chromatin fraction significantly decreased over time (Fig. 11, *D* and *E*). In parallel, we observed a progressive increase in RALY in the cytosolic fraction. The same result was observed when we incubated the cells with both ActD and the proteasome inhibitor MG132 (supplemental Fig. S4*A*), indicating that RALY had shifted from the nucleus to the cytoplasm and was not degraded by the proteasome and *de novo* synthesized to remain outside the nucleus. The inhibition of proteasome activity by MG132 was confirmed by the accumulation of ubiquitin in the cytosolic fraction (supplemental Fig. S4*B*). These results show that RALY localizes on transcriptionally active chromatin in a transcription-dependent manner and that the inhibition of transcription leads to a shuttling of RALY from the nuclear compartment to the cytoplasm. Taken together, these data demonstrating that RALY interacts with chromatin better characterize the direct role of RALY in gene expression regulation. Further experiments will be necessary to study this novel feature of RALY from the mechanistic point of view.

Discussion

The RNA-binding protein RALY has been described as interacting with numerous mRNAs to regulate the expression of specific transcripts. Moreover, the down-regulation of RALY is associated with reduced cell proliferation (32). Here we studied the association of RALY with cell cycle progression in greater detail. Our microarray analysis detected an altered expression of several transcription–, cell proliferation–, and cell cycle–related genes and revealed enrichment of members of the E2F transcription factors family and of cell cycle–related targets of the E2F family in the down-regulated genes upon RALY silencing (supplemental Table S1 and Fig. 3*A*). The family of the E2F transcription factors comprises eight members that regulate

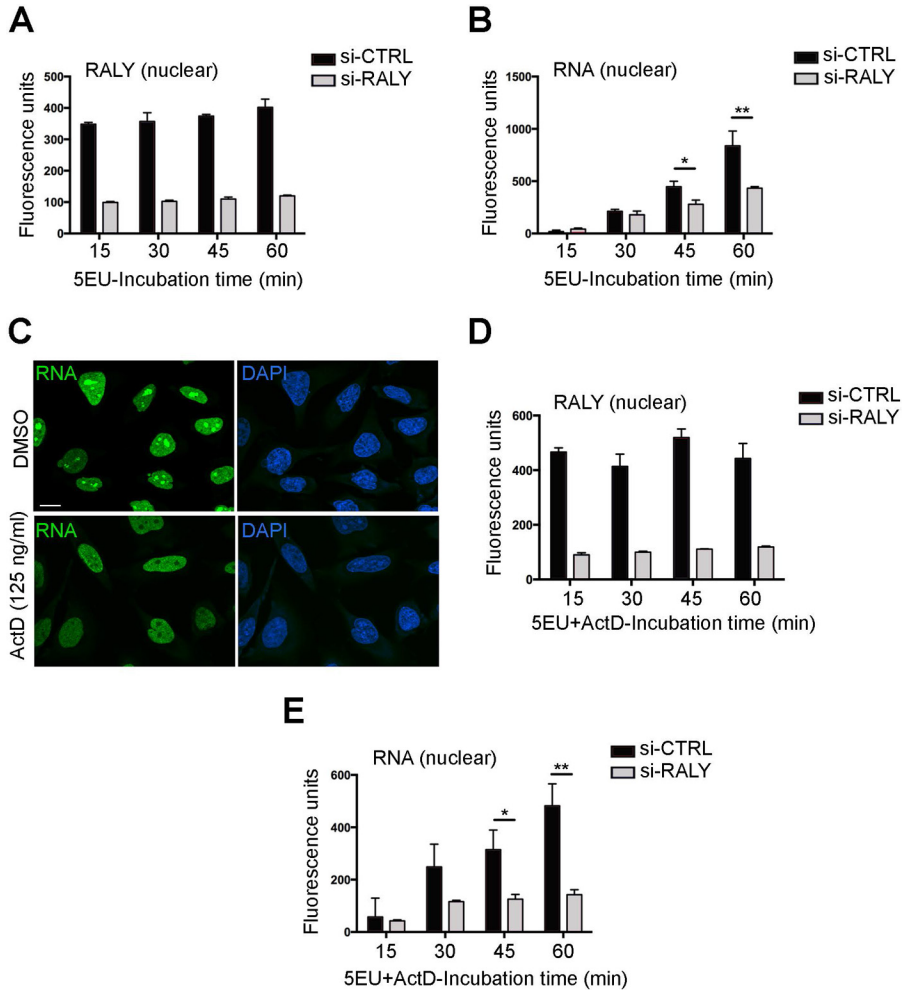

Figure 7. The down-regulation of RALY impairs RNAPII-dependent transcription. HeLa cells were transfected with either si-RALY or si-CTRL for 72 h. The cells were incubated successively with 5-EU (*A* and *B*) or 5-EU plus ActD (125 ng/ml) (*D* and *E*) for 0, 15, 30, 45, and 60 min. The down-regulation of RALY in the nucleus was verified by immunostaining with anti-RALY antibody (*A* and *D*). The amount of newly synthesized RNA was measured with a high-throughput fluorescence microscope after staining the incorporated 5-EU with the fluorescent molecule 5-FAM (*B* and *E*). In both the ActD-treated and untreated conditions, the levels of newly synthesized RNA show a slower increase over time in si-RALY cells compared with si-CTRL cells. The absence of RALY affects RNA polymerase II-dependent transcription. All of the *graphs* represent the mean of three independent experiments ± S.D. The *p* value was calculated using an unpaired two-tailed *t* test (*, $p < 0.05$; **, $p < 0.01$) between the respective samples of si-RALY– and si-CTRL–transfected cells. *C*, HeLa cells were incubated with 5-EU and treated with ActD (125 ng/ml) or DMSO for 1 h. Newly synthesized RNA was stained with 5-FAM and RALY through immunofluorescence with anti-RALY antibody. The mild ActD treatment only inhibited RNA polymerase I, abrogating the synthesis of RNA in the nucleoli. *Scale bar* = 10 μm.

cell physiology by either promoting or repressing cell cycle progression (47). Interestingly, all of the cell cycle–promoting E2Fs (E2F1–3) were found to be down-regulated upon RALY silencing in our microarray experiments (supplemental Table S1). We focused on E2F1, a well-known marker of cell proliferation and promoter of the S phase, which can also induce apoptosis through different p53-dependent and -independent mechanisms (35, 45, 67, 68). The overexpression of E2F1 has been reported in numerous types of cancer, and its ectopic expression was described to drive S-phase entry in quiescent cells and hyperplasia (48, 69). We show that RALY interacts with and stabilizes *E2F1* mRNA, consequently regulating the amount of E2F1 protein within the cell (Figs. 3, *D* and *E*, 4, and 5*A*). E2F1, together with its activating partner transcription factor DP1 (TFDP1), is normally kept in an inactivated state by the retinoblastoma protein (Rb) and is released at the G_1/S-phase transition after the CDK-mediated phosphorylation of Rb. The E2F1–TFDP1 complex will induce the expression of S phase–promoting factors, such as cyclin E1 and E2 (CCNE). In a positive feedback loop, CCNE will induce the further phosphorylation of Rb, consequently increasing the levels of free E2F1–TFDP1 complexes (70–72). A decreased expression of E2F1 therefore depotentiates the G_1/S-phase transition, lowering the expression of proliferation-promoting genes such as *CCNE* (70).

Consequently, we observed a lower expression of direct targets of E2F1 transcriptional control activity in RALY– down-regulated cells such as *CCNE1*, *CCNE2, CDC25A, CDK1*, and *CCNB1* (Fig. 2, *A* and *B*) (37, 38, 70, 72–74). Except for *CDC25A*, the other mRNA targets were also detected in the RIP-seq analysis of MCF7 cells by Rossi *et al.* (32). Although we did not validate these direct interactions in HeLa cells, we did not observe any adverse effect on their stability upon RALY down-regulation (data not shown). Thus, we cannot exclude the possibility that, together with E2F1 down-regulation, the absence of a direct interaction with RALY might also affect their

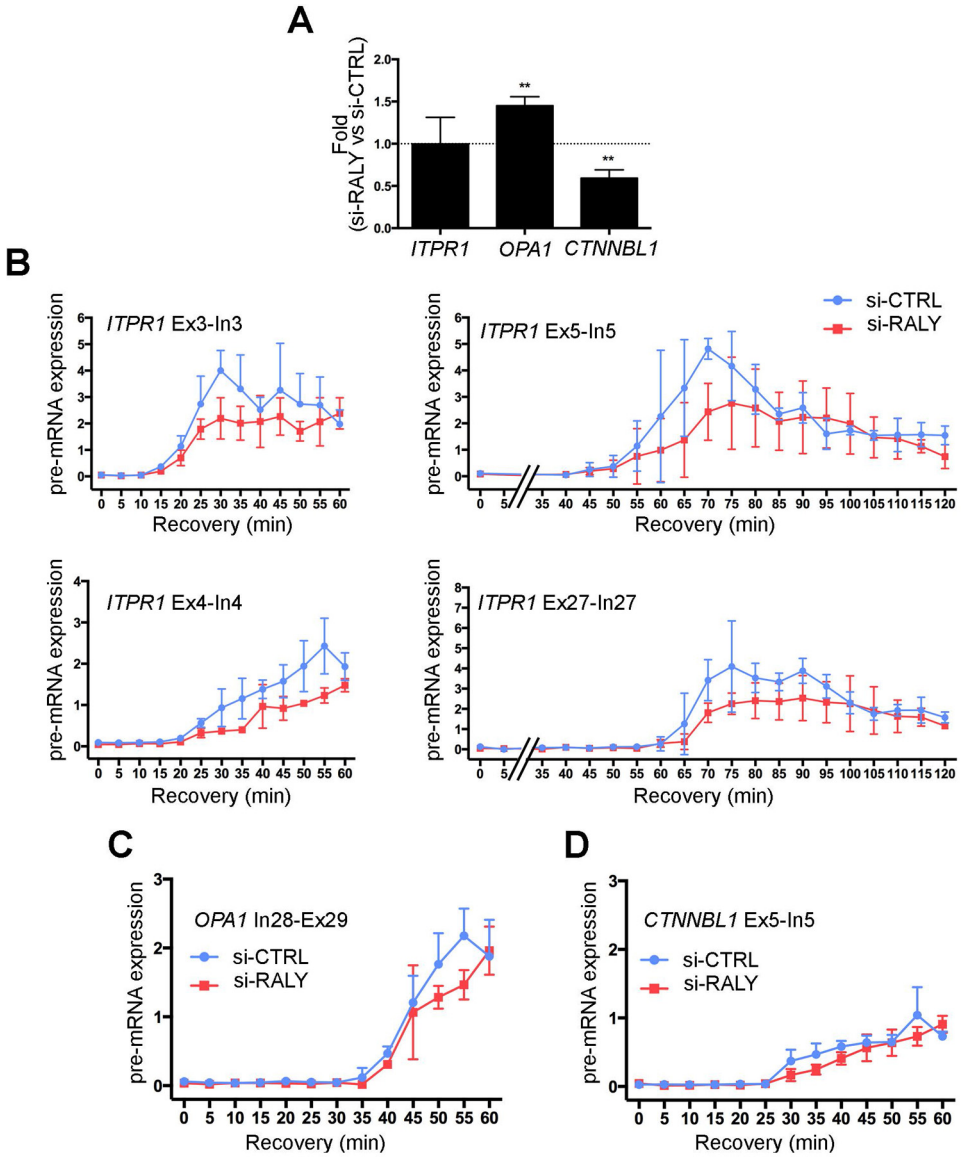

E

Gene Region	Length (kb)	Time to transcribe (min)		Elongation rate (kb/min)	
		si-CTRL	si-RALY	si-CTRL	si-RALY
ITPR1 Ex1-Ex3	23.5	10	10	2.32	2.32
ITPR1 Ex1-Ex4	28	15	15	1.86	1.86
ITPR1 Ex1-Ex5	133	40	40	3.33	3.33
ITPR1 Ex1-Ex27	190	55	55	3.46	3.46
OPA1 Ex1-Ex29	100	30	35	3.33	2.86
CTNNBL1 Ex1-Ex5	64	25	25	2.5	2.5
		Average elongation rate		**2.8±0.66**	**2.72±0.61**

Figure 8. Analysis of the elongation rate of RNAPII. *A*, HeLa cells were transfected with either si-RALY si-CTRL for 72 h. The expression level of *ITPR1*, *OPA1*, and *CTNNBL1* mRNAs was quantified by qRT-PCR and normalized on *GAPDH*. The level of *ITPR1* mRNA did not change significantly, whereas *OPA1* and *CTNNBL1* levels, respectively, increased and decreased in the absence of RALY compared with control cells. The *graph* shows the mean of three independent experiments ± S.D. The *p* value was calculated using an unpaired two-tailed *t* test between si-RALY– and si-CTRL–transfected cells (**, $p < 0.01$). *B–D*, HeLa cells transfected either with si-RALY or si-CTRL siRNA for 72 h were treated with 100 μM DRB for 3 h to block RNAPII activity. After washing with PBS, the cells were incubated in DMEM to recover transcription. Successively, total RNA was collected at 5-min intervals. qRT-PCR analysis with different exon-intron primer pairs for *ITPR1* (*B*), *OPA1* (*C*), and *CTNNBL1* (*D*) pre-mRNAs was used to measure RNAPII elongation rate. The pre-mRNA expression values are plotted relative to the expression level of the untreated controls, which was set to 1 in all experiments. RALY did not impair the RNAPII elongation rate. *E*, the *table* depicts the calculated elongation rate of RNAPII along the analyzed genes for both si-RALY– and si-CTRL–transfected cells. The down-regulation of RALY did not impair RNAPII elongation rate.

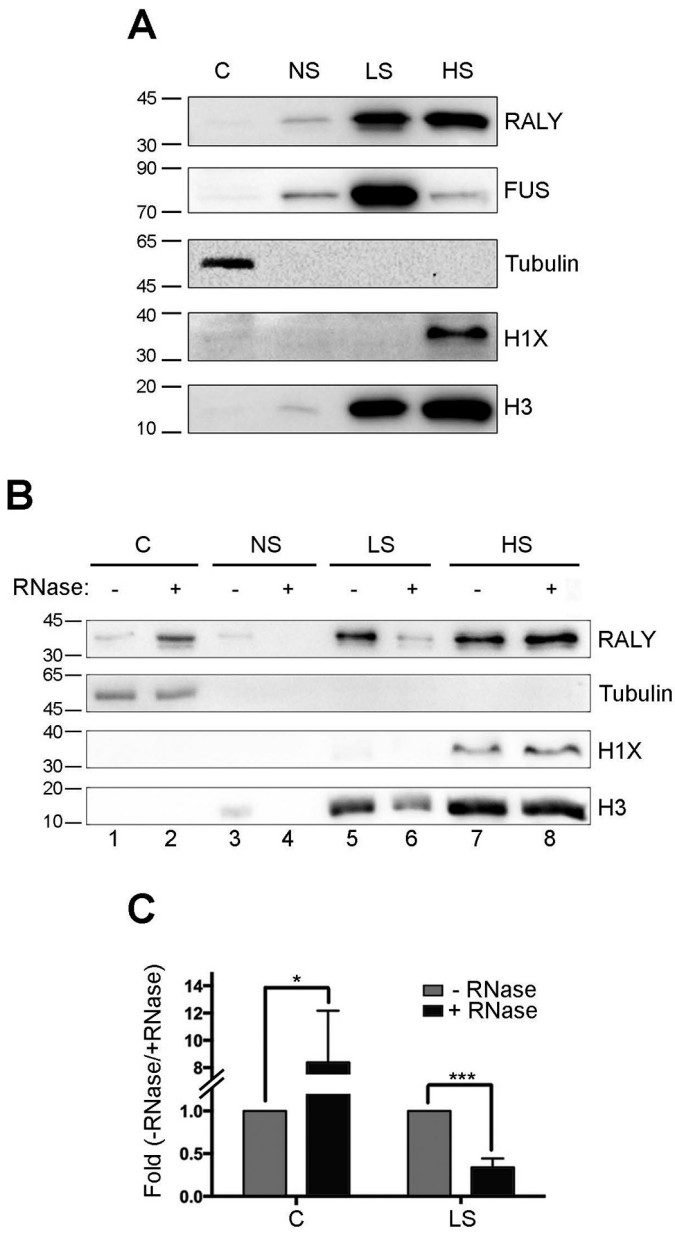

Figure 9. RALY is associated with chromatin. *A*, HeLa cell lysates were fractionated into cytosolic (*C*), nuclear-soluble (*NS*), low-salt–soluble chromatin (*LS*), and high-salt–soluble chromatin (*HS*) fractions. Each fraction was subjected to SDS-PAGE and Western blot analysis with the indicated antibodies. Endogenous RALY is faintly present in the cytosolic and nuclear-soluble fractions and enriched in both the low-salt– and high-salt–soluble fractions. FUS was analyzed to compare the behavior of RALY with a known hnRNP associated with chromatin. *B*, the distribution of endogenous RALY was examined by the fractionation method described in *A* either in the presence (−RNase) or absence of RNA (+RNase). In the absence of RNA, RALY decreases in the low-salt–soluble fraction and consequently increases in the cytosolic fraction. *C*, the levels of RALY were quantified by band densitometry analysis. The *graphs* show the mean values of three independent experiments and compare the level of RALY in the presence and absence of RNA in cytosolic and low-salt–soluble fractions. *Bars* represent mean ± S.D. The *p* value was calculated using an unpaired two-tailed *t* test (*, $p < 0.05$; ***, $p < 0.001$).

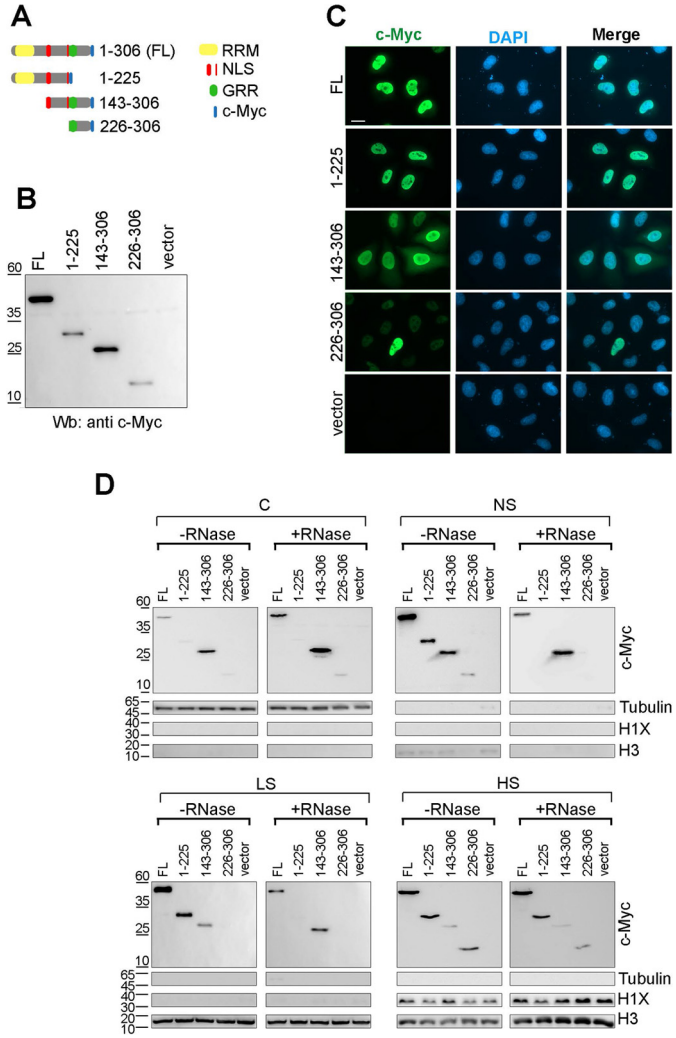

Figure 10. RALY interacts with nuclear components using either the N- or C-terminal region. *A*, schematic representation of c-Myc–tagged RALY constructs. *B*, C-Myc–tagged RALY constructs were transfected in HeLa cells for 24 h. Total lysates were subjected to SDS-PAGE and Western blot analysis with anti-c-Myc antibody. *C*, the cellular localization of RALY–c-Myc mutants was verified after immunofluorescence with anti-c-Myc antibody and DAPI staining. All of the recombinant fragments localized inside the nucleus. However, fragment(143–306) is also in the cytoplasm. *Scale bar* = 10 μm. *D*, RALY–c-Myc constructs were transfected in HeLa cells for 24 h, and the lysates were fractionated into cytosolic (*C*), nuclear-soluble (*NS*), low-salt–soluble chromatin (*LS*), and high-salt–soluble chromatin (*HS*) fractions. Each fraction was subjected to SDS-PAGE and Western blot analysis with the indicated antibodies. Both the N- and C-terminal regions of RALY can mediate an interaction with nuclear-soluble components and transcriptionally active chromatin (*LS*). In particular, the interactions made by RALY through the N-terminal RRM (construct(1–225)) in the nuclear-soluble and low-salt–soluble chromatin fractions are RNA-dependent.

expression. In fact, even though preliminarily, we observed that the loss of a direct interaction between RALY and mRNA could be associated with the down-regulation of the target mRNA (Fig. 1*E*).

Our observation of the down-regulation of E2F1, together with the lower expression of numerous transcription– and cell proliferation–promoting factors (Fig. 2*A* and supplemental Table S1), explains the decreased cell proliferation and stall in the G_1 phase of cells lacking RALY expression (Fig. 6, *A* and *B*, and supplemental Fig. S2) and the diminished RNAPII-dependent transcription in RALY-silenced cells (Fig. 7, *B* and *E*, and supplemental Fig. S3). In this view, the two processes are directly impaired by the down-regulation of the respective activating factors in response to RALY silencing, and they also mutually affect each other. RALY therefore can be classified as a novel indirect regulator of transcription and cell cycle progression. Further experiments will be necessary to better

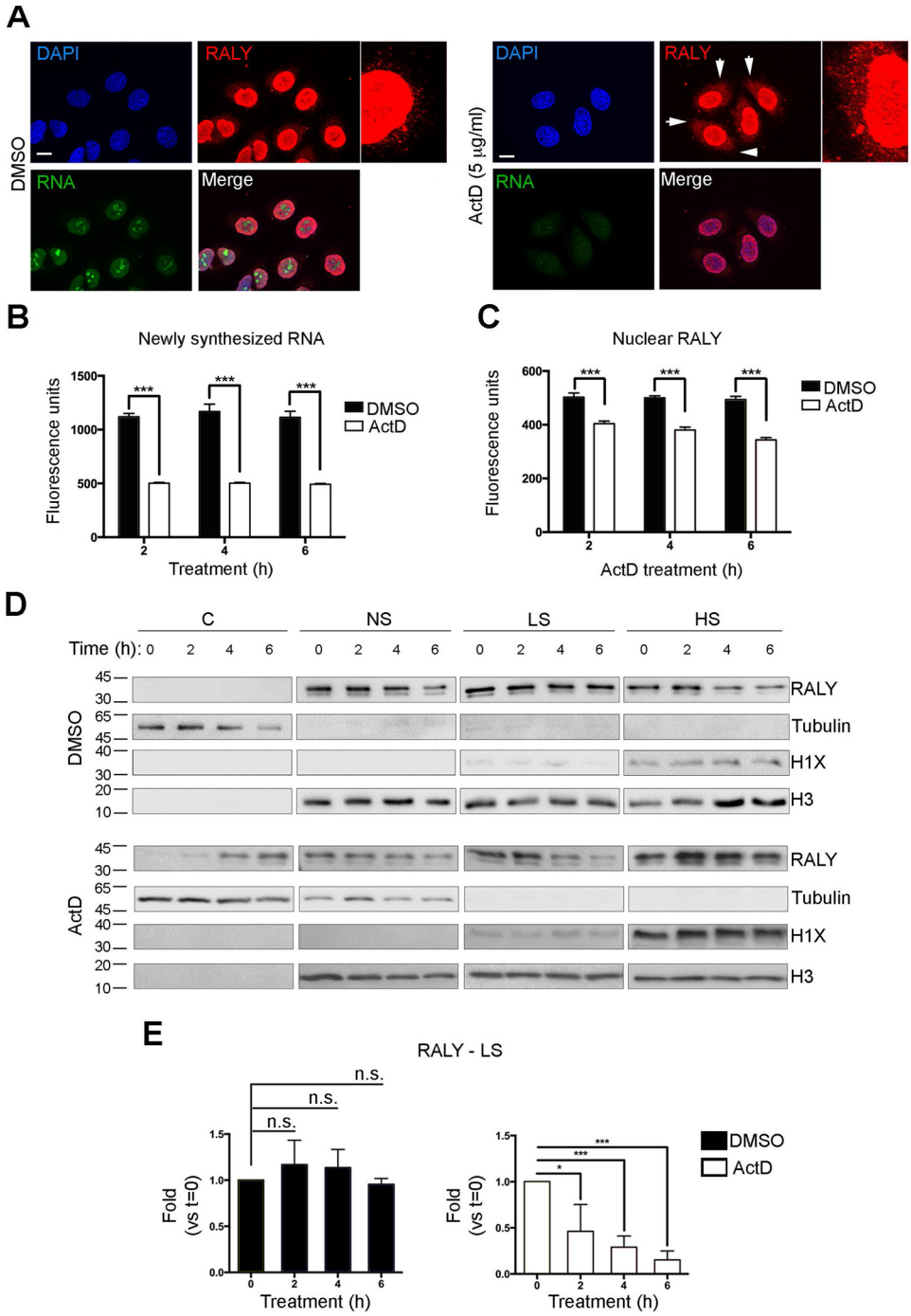

Figure 11. The localization of RALY is dependent on active transcription. *A*, HeLa cells were treated with 5-EU and either ActD (5 μg/ml) or vehicle (DMSO) for 2 h. RALY was stained with anti-RALY antibody and RNA with 5-FAM. After ActD treatment, there is a higher presence of RALY in the cytoplasm compared with the DMSO-treated cells (*arrowheads*). *Scale bar* = 10 μm. *B* and *C*, HeLa cells were treated with 5-EU plus either ActD (5 μg/ml) or vehicle (DMSO) for 2, 4, or 6 h, and the amount of nuclear newly synthesized RNA (*B*) and nuclear RALY (*C*), respectively, were assessed after staining with 5-FAM and after immunofluorescence with anti-RALY antibody using a high-throughput fluorescence microscope. The *graphs* represent the mean of three independent experiments and highlight the absence of new RNA synthesis (*B*) and the decrease of nuclear RALY (*C*) in HeLa cells treated with ActD. In *B*, the remaining RNA signal was considered background noise. The *p* value was calculated using an unpaired two-tailed *t* test comparing the 5-FAM signal (*B*) and the nuclear level of RALY (*C*) of the treated cells (ActD or DMSO) with the respective untreated sample ($t = 0$) (***, $p < 0.001$). *D*, HeLa cells were treated with either ActD (5 μg/ml) or DMSO for 0, 2, 4, or 6 h. At each time point, the cells were fractionated into cytosolic (*C*), nuclear-soluble (*NS*), low-salt–soluble chromatin (*LS*), and high-salt–soluble chromatin (*HS*) fractions. Then, each fraction was subjected to SDS-PAGE and Western blot analysis with the indicated antibodies. Along with the ActD treatment, the amount of RALY decreases in the low-salt–soluble chromatin fraction and in parallel increases in the cytosolic fraction. *E*, the levels of RALY in the low-salt–soluble chromatin fraction were quantified by band densitometry analysis. The *graphs* represent the mean of three independent experiments and highlight the significant decrease in RALY in the low-salt–soluble chromatin fraction during ActD treatment (*right graph*) compared with DMSO treatment (*left graph*). The *p* value was calculated comparing the level of RALY in the low-salt–soluble chromatin fraction of the treated cells with the respective untreated samples ($t = 0$) using an unpaired two-tailed *t* test (*, $p < 0.05$; ***, $p < 0.001$). *n.s.*, not statistically significant.

understand the whole spectra of molecular functions of RALY. For example, the analysis of nuclear and cytoplasmic RNAs could clarify whether the RALY-mediated stabilization of *E2F1* mRNA, and in general of other transcripts, occurs at the level of nascent or rather mature RNA. Nevertheless, an involvement of RALY in the 3′-end processing and termination can be hypothesized. In fact, Fasken *et al*. (75) observed functional homologies between human RALY and the yeast protein Nab3, an RNA-binding protein involved in the exosome-mediated processing, termination, and degradation of noncoding RNAs (ncRNA). Nab3 and RALY share 31% sequence homology in the RRM and a certain degree of similarity also in the C-terminal region, and the expression of RALY in Nab3-negative cells rescued the thermosensitive yeast phenotype. Interestingly, to be efficient, both proteins need a functional RRM (75). RALY could be involved in the 3′-end processing of coding as well as noncoding RNAs, ultimately affecting RNA stability, but further experiments are needed to better elucidate this possibility. Recently, RALY was described as having a direct role in regulating the splicing of the protein arginine methyltransferase 1 (*PRMT1*) mRNA, coding for a factor involved in the post-translational methylation of proteins and found to be aberrantly regulated in different cancers (76). A spliced isoform of PRMT1 that includes the alternative second exon (PRMT1v2) was found to be up-regulated in breast cancer and was correlated with high aggressiveness (77). Interestingly, *PRMT1* mRNA is a direct target of RALY and RALY knockdown determines a significant decrease in PRMT1v2 mRNA and protein inside the cell, consequently determining a reduction of invasiveness. The overexpression of PRMT1v2 in RALY–down-regulated cells rescues the aggressive phenotype of the breast cancer cells (76). These results demonstrate the direct involvement of RALY in the splicing of a specific mRNA with consequent effects on cell phenotype. It is therefore possible that RALY caused part of the effects observed in our study by modulating the splicing of specific factors. Further experiments will be performed to study the involvement of RALY in splicing regulation.

Our results characterized the effect of RALY on cellular physiology by the regulation of its target mRNAs. RALY was recently characterized as binding gene promoters to act as a transcriptional co-factor together with the ncRNA *Lexis* in the cholesterol biogenesis pathway in mouse liver (34). This prompted us to characterize in detail the association of RALY with chromatin. Here, we have demonstrated that RALY interacts with transcriptionally active chromatin and that the association is partially abrogated upon RNA degradation (Fig. 9, *B* and *C*). Based on our results, we propose that the association of RALY with transcriptionally active chromatin is mediated by two types of interaction: one, an RNA-dependent interaction through the RRM domain to bind and process RNAs possibly in synergy with other factors; and another, an RNA-independent interaction mediated by the C-terminal domain (Fig. 10*D*). Interestingly, the fragment of RALY (amino acids 143–306) involved in the RNA-independent interaction with chromatin contains a basic leucine zipper–like motif (bZLM) typical of DNA-binding proteins, more precisely between the amino acids 146–214 (25, 34). Because the construct containing only the GRR (glycine-rich region) domain was not found on transcriptionally active chromatin, we concluded that the bZLM is necessary for the RNA-independent association of RALY with active chromatin. This interaction may allow RALY to function as a transcriptional co-factor (34), by binding DNA, but could also serve to anchor RALY on chromatin to allow its N-terminal RRM domain to contact RNAs. Further experiments will better characterize the function of the two diverse bindings of RALY to transcriptionally active chromatin.

To gain more information about the cellular distribution of RALY, we analyzed the localization of the RBP FUS/TLS, also classified as hnRNP-P2, finding that the two RBPs share the localization in the nuclear-soluble and the transcriptionally active chromatin fractions (Fig. 9*A*) (13, 64). FUS is a well-studied RBP because of its association with multiple diseases, particularly those affecting the nervous system, and has different biological functions, including transcription regulation, RNA biogenesis and post-transcriptional modification (65, 66, 78). Further experiments will explore the interaction and possible shared functions between RALY and FUS.

RALY showed a partial RNA dependence in its interaction with chromatin when RNA was degraded *in vitro*. *In vivo*, the presence of RNA on chromatin is mainly due to ongoing transcription, and the inhibition of RNA synthesis may lead to changes in the association of RBPs with chromatin. treatment with ActD induced a progressive delocalization of RALY from transcriptionally active chromatin to the cytoplasm, suggesting that the interaction of RALY with this fraction of chromatin requires the active synthesis of new transcripts (Fig. 11, *D* and *E*). The transcription block might abrogate the dynamic recruitment of RALY on chromatin, disrupting the existing interactions and preventing the formation of new associations, but also make the RALY pool intended to interact with RNA unnecessary. As a consequence of the transcription block, RALY migrates from the nucleus to the cytoplasm. Whether the RNA-dependent and -independent interactions are equally affected by the block of transcription remains to be elucidated. Taken together, our results characterize RALY as an indirect regulator of cell proliferation and transcription and better define the direct interaction of RALY with chromatin, making the transcriptional control activity of RALY an interesting topic for study.

Experimental procedures

Cell cultures and transient transfections

HeLa cells and MCF7 were grown in DMEM supplemented with 10% FBS as described previously (79). HPNE cells were grown in 75% DMEM, 25% M3 base, 5% FCS, 10 ng/ml human recombinant EGF, and 750 ng/ml puromycin. MCF10A cells were cultured in DMEM/F12 Ham's mixture supplemented with 5% equine serum, 20 ng/ml EGF (Sigma), 10 μg/ml insulin (Sigma), 0.5 mg/ml hydrocortisone (Sigma), 100 ng/ml cholera toxin (Sigma), 100 units/ml penicillin, and 100 μg/ml streptomycin. The cells were cultured in an incubator at 37 °C with 5% CO_2. The stable RALY knock-out HeLa cells were generated by CRISPR/Cas9 technology as described previously (32).

Plasmid transfection was performed using the TransIT transfection reagent (Mirus Bio LLC) according to the manu-

facturer's protocols. The transfections of ON-TARGETplus SMARTpool siRNAs and control siRNAs (Thermo Fisher Scientific) were performed with the INTERFERin transfection reagent (Polyplus-transfection) according to the manufacturer's protocols.

qRT-PCR

Total RNA was purified from cells using TRIzol reagent (Thermo Fisher Scientific) and retrotranscribed using the RevertAid first-strand cDNA synthesis kit (Thermo Fisher Scientific). The KAPA SYBR FAST qPCR kit (KAPA Biosystems) was used for the qRT-PCR. All primers were purchased from Integrated DNA Technologies and are listed in supplemental Table S3. The samples were incubated in a Bio-Rad CFX96 Thermo Cycler for 40 cycles, and the results were analyzed with Bio-Rad CFX Manager, version 2.1. The relative expression was calculated according to the $2^{-\Delta\Delta}C_t$ method.

Constructs

Reverse transcription was performed on total RNA isolated from HeLa cells using the TRIzol reagent. Human RALY cDNA was amplified with Phusion high-fidelity DNA polymerase (New England Biolabs) and then cloned in-frame with the c-Myc/DDK tag (pCMV6-Entry Vector, Origene). The sequences of the primers are listed in supplemental Table S3.

Preparation of cell extracts and Western blot analysis

The cells were washed with prewarmed PBS and lysed in lysis buffer (0.1% Triton X-100, 0.5% Nonidet P-40, 150 mM NaCl, 20 mM Tris-HCl, pH 8, plus protease inhibitor mixture (Roche Applied Science), including 1 mM PMSF). Equal amounts of proteins were separated on 12% SDS-PAGE and blotted onto nitrocellulose (GE Healthcare). Western blotting was performed by probing with the following primary antibodies: rabbit polyclonal anti-RALY (A302-070A, Bethyl Laboratories), mouse monoclonal anti-c-Myc (M4439, Sigma Aldrich), rabbit polyclonal anti-H1X (ab31972, Abcam), mouse monoclonal anti-β-tubulin (sc-53140, Santa Cruz Biotechnology), rabbit polyclonal anti-FUS/TLS (ab2349, Abcam), rabbit polyclonal anti-H3 (ab1791, Abcam), mouse monoclonal anti-E2F1 (sc-251, Santa Cruz Biotechnology), mouse monoclonal anti-ubiquitin (3936, Cell Signaling Technology), and mouse monoclonal anti-GAPDH (sc-32233, Santa Cruz Biotechnology). HRP-conjugated goat anti-mouse and anti-rabbit antibodies (Santa Cruz Biotechnology) were used as secondary antibodies.

Micrococcal nuclease cell fractionation

Cell fractionation was performed as described by Yang *et al.* (13). Briefly, HeLa cell pellets were incubated for 10 min on ice in nucleus separation buffer (NSB) (10 mM KCl, 1.5 mM $MgCl_2$, 0.34 M sucrose, 10% glycerol, 1 mM DTT, and 0.1% Triton X-100) supplemented with protease inhibitors (Roche Applied Science) and RNase inhibitors (New England Biolabs) depending on the experiment. For RNase treatment, RNase A (100 μg/ml) was added to NSB, and after 10 min on ice, both the RNase A–treated and untreated extracts were incubated at 37 °C for 10 min. The samples were then centrifuged at 1400 × *g* at 4 °C for 10 min to pellet the nuclei. The supernatant (cytosolic fraction) was collected, and the pellet containing the nuclei was resuspended in NSB supplemented with 1 mM $CaCl_2$ and 2000 units/ml micrococcal nuclease (MNase, New England Biolabs) and incubated at 37 °C for 10 min. EGTA was then added to arrive at a 2 mM concentration to stop the MNase reaction. The samples were centrifuged at 1400 × *g* at 4 °C for 10 min to pellet chromatin. The supernatant (nuclear soluble fraction) was collected, and chromatin was resuspended in NSB supplemented with 150 mM NaCl. The tubes were left in rotation at 4 °C for 2 h. The samples were then centrifuged at 1400 × *g* at 4 °C for 10 min to pellet chromatin again. The supernatant was collected (low-salt–soluble fraction, transcriptionally active chromatin), and the remaining pellet was dissolved in NSB supplemented with 600 mM NaCl. The samples were left in rotation at 4 °C overnight. The tubes were finally centrifuged at 1400 × *g* at 4 °C for 10 min to pellet the insoluble fraction of chromatin, and the last supernatant was collect (high-salt–soluble fraction, transcriptionally inactive chromatin). After the supernatant collections, every fraction was clarified with a centrifugation at 16,400 × *g* at 4 °C for 2 min.

RNA synthesis assay

HeLa cells were grown for 24 h to obtain 70–80% confluence. The cells were incubated in complete DMEM supplemented with 0.5 mM 5-EU (Jena Bioscience) for the desired amount of time. When required, actinomycin D was added at the concentration of 125 ng/ml at the same moment. The cells were then fixed for 30 min at room temperature in fixing solution (125 mM Pipes, pH 6.8, 10 mM EGTA, 1 mM $MgCl_2$, 0.2% Triton X-100, and 3.7% formaldehyde). Click reaction with 5-FAM-azide (5-FAM, Jena Bioscience) was performed in staining solution (100 mM Tris, pH 8.5, 1 mM $CuSO_4$, 10 μM 5-FAM, and 100 mM ascorbic acid (in water)). Finally, the cells were washed three times in TBS supplemented with 0.5% Triton X-100. Staining of the proteins was achieved by incubating the cells in blocking solution according to the immunocytochemistry protocol described below.

RNA pulldown

RNA pulldown was performed as described previously by Rossi *et al.* (32). Briefly, wild-type or mutant probes (50 pmol) were incubated with 35 μl of streptavidin-coupled Dynabeads (Thermo Fisher Scientific) for 20 min at room temperature in RNA capture buffer (20 mM Tris, pH 7.5, 1 M NaCl, 1 mM EDTA). HeLa cells were washed with PBS and then lysed with the lysis buffer (20 mM Tris, pH 7.5, 50 mM NaCl, 2 mM $MgCl_2$, and 0.1% Tween 20). The lysate (200 μg) was incubated with biotinylated RNA probes coupled to streptavidin–Dynabeads for 1 h at 4 °C under rotation. Dynabeads were then washed three times with washing solution (20 mM Tris, pH 7.5, 10 mM NaCl, and 0.1% Tween 20), solubilized in Laemmli reducing buffer, and boiled for Western blot analysis.

Immunocytochemistry and fluorescence microscopy

Cells were washed in prewarmed PBS and then fixed in 4% paraformaldehyde for 15 min at room temperature. Immunocytochemistry was carried out as described previously (32). The

following primary antibodies were used: rabbit polyclonal anti-RALY (A302-070A, Bethyl Laboratories), mouse monoclonal anti-c-Myc (M4439, Sigma Aldrich). Alexa 594– and Alexa 488–coupled goat anti-mouse and anti-rabbit IgG were used as secondary antibodies (Santa Cruz Biotechnology). Microscopy analysis was performed using the Zeiss Observer Z.1 microscope implemented with the Zeiss ApoTome module. Pictures were acquired using Zen Blue imaging software package (Zeiss) and assembled with Adobe Photoshop CS6. Images were not modified other than by adjustments to the level, brightness, and magnification.

RNA immunoprecipitation

RIP was performed as reported by Keene *et al.* (80) with some modifications. In brief, 4×10^7 cells were grown in 15-cm culture dishes and irradiated once with 150 mJ/cm^2 at 254 nm using a UVLink UV cross-linker (Uvitec Cambridge). The cells were lysed in lysis buffer (10 mM HEPES, pH 7.4, 100 mM KCl, 5 mM $MgCl_2$, 0.5% Nonidet P-40, 1 mM DTT, 100 units/ml RNase Out, and protease inhibitor mixture) for 3 h at −80 °C and centrifuged at 10,000 × *g* for 20 min at 4 °C. Then the supernatants were precleared with 20 μl of A/G–magnetic beads for 1 h at 4 °C. Successively, the supernatants were incubated for 4 h at 4 °C with protein A/G–magnetic beads coated either with antibody anti-RALY (A302-069A, Bethyl Laboratories) (3 μg) or with normal rabbit IgG polyclonal antibody (Millipore). The beads were then washed three times with NT2 buffer (50 mM Tris-HCl, pH 7.5, 300 mM NaCl, 1 mM $MgCl_2$, 0.05% Nonidet P-40, and 1% urea). The RNA was isolated with TRIzol and processed for qRT-PCR analysis. The primers are shown in supplemental Table S3.

Real-time cell analysis

The cell proliferation assay using the xCELLigence system (Roche Applied Science) was performed according to the manufacturer. Briefly, 4×10^4 RALY KO and PX330 cells were seeded into each well of a specific xCELLigence E-plate. Cell proliferation was monitored by the instrument by measuring the impedance at the bottom of the wells for 3 days with detections every 15 min. The proliferation signals were normalized on the signals acquired at 10 h post seeding.

Cell cycle distribution analysis

Cell cycle distribution was analyzed as described by Massey (58). Briefly, 10^4 RALY KO and PX330 cells were seeded into a 96-well plate and grown for 24 h. Cells were incubated successively in DMEM plus 10 μM 5-ethynyl-deoxiuridine and successively treated for Click-iT reaction as described above. Processed cells were analyzed successively with the high-content imaging system Operetta, as described by Massey (58).

RNA polymerase II elongation rate

RNA polymerase II elongation was monitored according to Singh and Padgett (60). Briefly, HeLa cells were grown in 6-well plates until 70% confluence and successively transfected with either si-CTRL or si-RALY. After 72 h, the cells were incubated for 3 h in Complete DMEM + 100 μM DRB to block RNAPII-dependent transcription. The cells were washed successively twice with ice-cold PBS and incubated with DMEM at 37 °C to reactivate transcription. Cells were then lysed at 5-min intervals using the lysis buffer of the High Pure isolation kit (Roche Applied Science), and total RNA was extracted. Reverse transcription was performed using the ImProm-II reverse transcription system (Promega). The analysis of pre-mRNA levels was done by quantitative real-time PCR using the primers listed in supplemental Table S3. For this analysis, the qRT-PCR results of the transfected cells (si-CTRL or si-RALY) not treated with DRB were used as reference values for the normalization of the transfected cells treated with DRB for 3 h and then allowed to recover transcription.

High-content analysis

HeLa cells were plated (1×10^4 cells/well) in 96-well plates (Corning) and transfected on the following day with either si-CTRL or si-RALY for 72 h. Then, depending on the experiment, the cells were either immunostained (for the experiment shown in Fig. 11) or incubated for different amounts of time with 0.5 mM 5-EU in warm DMEM to mark the newly synthesized RNA and successively stained with 5-FAM through Click-iT reaction (see "RNA synthesis assay" above) followed by immunocytochemistry, starting from the blocking step, as described above (for the experiment in Fig. 7). Plates were imaged on the high-content imaging system Operetta™ (PerkinElmer). In each of the 4 wells for every condition, images were acquired in five preselected fields with a LWD (long working distance) 20× objective over three channels, with λ = 380 nm excitation/λ = 445 nm emission for DAPI, λ = 495 nm excitation/λ = 519 nm emission for Alexa Fluor 488 or 5-FAM, and λ = 535 nm excitation/λ = 615 nm emission for Alexa Fluor 594. For feature extraction, the images were analyzed using Harmony software, version 4.1 (PerkinElmer). Individual cell nuclei were segmented based on DAPI staining. For the Click-iT experiment (Fig. 7) the Select Population algorithm allowed us to identify the subpopulation of silenced cells for RALY by setting a fluorescence intensity threshold on the Alexa Fluor 594 signal. The 5-FAM signal was then measured only in the cells evaluated as silenced for RALY.

Microarray analysis

HeLa cells were transfected for 72 h with either si-CTRL or si-RALY as described above, and total RNA was extracted using the High Pure isolation kit (Roche Applied Science). Samples were prepared for hybridization following the Affymetrix WT PLUS reagent kit protocol. The amplified and labeled samples were hybridized to the Affymetrix GeneChip human transcriptome array 2.0 (Affymetrix, Santa Clara, CA). Arrays were washed and stained using the Affymetrix Fluidics Station 450, and scanned in the Affymetrix GeneArray 3000 7G scanner. The experiment was performed in biological triplicate.

The CEL files resulting from the GeneChip analysis were analyzed with Affymetrix transcriptome analysis console (TAC) 3.1 and the Bioconductor library of biostatistical packages (http://www.bioconductor.org/).[4] (82). Raw data were

[4] Please note that the JBC is not responsible for the long-term archiving and maintenance of this site or any other third party hosted site.

preprocessed and normalized using the robust multichip analysis (RMA) method. Gene average intensities were determined with Tukey's biweight average algorithm using Affymetrix default analysis settings. Differentially expressed genes (DEG) upon RALY silencing were determined adopting a double threshold based on statistical significance (unpaired one-way analysis of variance, FDR < 0.05) and log2 fold change (>0.5 for up-regulated genes and <-0.5 for down-regulated genes).

The frequencies of RALY RIP-seq targets among DEGs were tested with the "test of equal or given proportions" implemented in R. The ClusterProfiler package was used for enrichment analysis of DEG lists using annotations from the Gene Ontology (http://www.geneontology.org),[4] KEGG (http://www.genome.jp/kegg/),[4] and REACTOME (http://www.reactome.org/)[4] databases. The significance of overrepresentation was determined using an FDR threshold of 0.05. GSEA was performed on ranked DEGs against the MSigDB hallmark collection of annotated gene sets (v 5.2) (81).

Author contributions—N. C., A. R., R. A. P., and P. M. designed the experiments. N. C. and A. R. conducted the experiments. L. G. contributed to the production of the constructs and participated in the experiments with recombinant proteins (Fig. 10). R. A. P. and J. S. contributed to the conception of Fig. 8 and designed the primers for the experiments depicted therein. TT analyzed the microarray data presented in Figs. 1 and 3. N. C., A. R., and P. M. wrote the paper. All authors analyzed the results and approved the final version of the manuscript.

Acknowledgments—We thank Drs. Valentina Adami and Michael Pancher (CIBIO-High Throughput Screening Core Facility) for technical assistance. We are grateful to Dr. Alessandro Provenzani for comments on the manuscript.

References

1. Sainsbury, S., Bernecky, C., and Cramer, P. (2015) Structural basis of transcription initiation by RNA polymerase II. *Nat. Rev. Mol. Cell Biol.* **16,** 129–143
2. Thomas, M. C., and Chiang, C. M. (2006) The general transcription machinery and general cofactors. *Crit. Rev. Biochem. Mol. Biol.* **41,** 105–178
3. Fredericks, A. M., Cygan, K. J., Brown, B. A., and Fairbrother, W. G. (2015) RNA-binding proteins: Splicing factors and disease. *Biomolecules* **5,** 893–909
4. Das, R., Yu, J., Zhang, Z., Gygi, M. P., Krainer, A. R., Gygi, S. P., and Reed, R. (2007) SR proteins function in coupling RNAP II transcription to pre-mRNA splicing. *Mol. Cell* **26,** 867–881
5. Fackelmayer, F. O., Dahm, K., Renz, A., Ramsperger, U., and Richter, A. (1994) Nucleic-acid-binding properties of hnRNP/SAF-A, a nuclear-matrix protein which binds DNA and RNA *in vivo* and *in vitro*. *Eur. J. Biochem.* **221,** 749–757
6. Takimoto, M., Tomonaga, T., Matunis, M., Avigan, M., Krutzsch, H., Dreyfuss, G., and Levens, D. (1993) Specific binding of heterogeneous ribonucleoprotein particle protein K to the human c-*myc* promoter *in vitro*. *J. Biol. Chem.* **268,** 18249–18258
7. Michelotti, E. F., Michelotti, G. A., Aronsohn, A. I., and Levens, D. (1996) Heterogeneous nuclear ribonucleoprotein K is a transcription factor. *Mol. Cell. Biol.* **16,** 2350–2360
8. Huang, Y. S., and Richter, J. D. (2004) Regulation of local mRNA translation. *Curr. Opin. Cell Biol.* **16,** 308–313
9. Norton, P. A. (1994) Alternative pre-mRNA splicing: Factors involved in splice site selection. *J. Cell Sci.* **107,** 1–7
10. Swinburne, I. A., Meyer, C. A., Liu, X. S., Silver, P. A., and Brodsky, A. S. (2006) Genomic localization of RNA binding proteins reveals links between pre-mRNA processing and transcription. *Genome Res.* **16,** 912–921
11. Cirillo, D., Marchese, D., Agostini, F., Livi, C. M., Botta-Orfila, T., and Tartaglia, G. G. (2014) Constitutive patterns of gene expression regulated by RNA-binding proteins. *Genome Biol.* **15,** R13
12. Rajagopalan, L. E., Westmark, C. J., Jarzembowski, J. A., and Malter, J. S. (1998) hnRNP C increases amyloid precursor protein (APP) production by stabilizing APP mRNA. *Nucleic Acids Res.* **26,** 3418–3423
13. Yang, L., Gal, J., Chen, J., and Zhu, H. (2014) Self-assembled FUS binds active chromatin and regulates gene transcription. *Proc. Natl. Acad. Sci. U.S.A.* **111,** 17809–17814
14. Castello, A., Fischer, B., Hentze, M. W., and Preiss, T. (2013) RNA-binding proteins in Mendelian disease. *Trends Genet.* **29,** 318–327
15. Lukong, K. E., Chang, K. W., Khandjian, E. W., and Richard, S. (2008) RNA-binding proteins in human genetic disease. *Trends Genet.* **24,** 416–425
16. Brinegar, A. E., and Cooper, T. A. (2016) Roles for RNA-binding proteins in development and disease. *Brain Res.* **1647,** 1–8
17. Cooper, T. A., Wan, L., and Dreyfuss, G. (2009) RNA and disease. *Cell* **136,** 777–793
18. Philips, A. V., and Cooper, T. A. (2000) RNA processing and human disease. *Cell. Mol. Life Sci.* **57,** 235–249
19. Meng, P., and Ghosh, R. (2014) Transcription addiction: Can we garner the yin and yang functions of E2F1 for cancer therapy? *Cell Death Dis.* **5,** e1360
20. Dreyfuss, G., Kim, V. N., and Kataoka, N. (2002) Messenger-RNA-binding proteins and the messages they carry. *Nat. Rev. Mol. Cell Biol.* **3,** 195–205
21. Chaudhury, A., Chander, P., and Howe, P. H. (2010) Heterogeneous nuclear ribonucleoproteins (hnRNPs) in cellular processes: Focus on hnRNP E1's multifunctional regulatory roles. *RNA* **16,** 1449–1462
22. Weighardt, F., Biamonti, G., and Riva, S. (1996) The roles of heterogeneous nuclear ribonucleoproteins (hnRNP) in RNA metabolism. *BioEssays* **18,** 747–756
23. Geuens, T., Bouhy, D., and Timmerman, V. (2016) The hnRNP family: Insights into their role in health and disease. *Hum. Genet.* **135,** 851–867
24. Krecic, A. M., and Swanson, M. S. (1999) hnRNP complexes: Composition, structure, and function. *Curr. Opin. Cell Biol.* **11,** 363–371
25. McAfee, J. G., Shahied-Milam, L., Soltaninassab, S. R., and LeStourgeon, W. M. (1996) A major determinant of hnRNP C protein binding to RNA is a novel bZIP-like RNA binding domain. *RNA.* **2,** 1139–1152
26. McCloskey, A., Taniguchi, I., Shinmyozu, K., and Ohno, M. (2012) hnRNP C tetramer measures RNA length to classify RNA polymerase II transcripts for export. *Science* **335,** 1643–1646
27. Ye, J., Beetz, N., O'Keeffe, S., Tapia, J. C., Macpherson, L., Chen, W. V., Bassel-Duby, R., Olson, E. N., and Maniatis, T. (2015) hnRNP U protein is required for normal pre-mRNA splicing and postnatal heart development and function. *Proc. Natl. Acad. Sci. U.S.A.* **112,** E3020–E3029
28. Kim, M. K., and Nikodem, V. M. (1999) hnRNP U inhibits carboxy-terminal domain phosphorylation by TFIIH and represses RNA polymerase II elongation. *Mol. Cell. Biol.* **19,** 6833–6844
29. Mikula, M., Bomsztyk, K., Goryca, K., Chojnowski, K., and Ostrowski, J. (2013) Heterogeneous nuclear ribonucleoprotein (hnRNP) K genome-wide binding survey reveals its role in regulating 3′-end RNA processing and transcription termination at the early growth response 1 (*EGR1*) gene through XRN2 exonuclease. *J. Biol. Chem.* **288,** 24788–24798
30. Rhodes, G. H., Valbracht, J. R., Nguyen, M. D., and Vaughan, J. H. (1997) The p542 gene encodes an autoantigen that cross-reacts with EBNA-1 of the Epstein Barr virus and which may be a heterogeneous nuclear ribonucleoprotein. *J. Autoimmun.* **10,** 447–454
31. Tenzer, S., Moro, A., Kuharev, J., Francis, A. C., Vidalino, L., Provenzani, A., and Macchi, P. (2013) Proteome-wide characterization of the RNA-binding protein RALY-interactome using the in *vivo*-biotinylation-pull-down-quant (iBioPQ) approach. *J. Proteome Res.* **12,** 2869–2884
32. Rossi, A., Moro, A., Tebaldi, T., Cornella, N., Gasperini, L., Lunelli, L., Quattrone, A., Viero, G., and Macchi, P. (2017) Identification and dynamic changes of RNAs isolated from RALY-containing ribonucleoprotein complexes. *Nucleic Acids Res.* **45,** 6775–6792

33. Pineda, G., Shen, Z., de Albuquerque, C. P., Reynoso, E., Chen, J., Tu, C. C., Tang, W., Briggs, S., Zhou, H., and Wang, J. Y. (2015) Proteomics studies of the interactome of RNA polymerase II C-terminal repeated domain. *BMC Res. Notes* **8,** 616
34. Sallam, T., Jones, M. C., Gilliland, T., Zhang, L., Wu, X., Eskin, A., Sandhu, J., Casero, D., Vallim, T. Q., Hong, C., Katz, M., Lee, R., Whitelegge, J., and Tontonoz, P. (2016) Feedback modulation of cholesterol metabolism by the lipid-responsive non-coding RNA LeXis. *Nature* **534,** 124–128
35. Whitfield, M. L., George, L. K., Grant, G. D., and Perou, C. M. (2006) Common markers of proliferation. *Nat. Rev. Cancer* **6,** 99–106
36. Lindqvist, A., Van Zon, W., Karlsson Rosenthal, C., Wolthuis, R. M. F., Rosenthal, C. K., and Wolthuis, R. M. (2007) Cyclin B1-Cdk1 activation continues after centrosome separation to control mitotic progression. *PLoS Biol.* **5,** 1127–1137
37. Nam, H. J., and van Deursen, J. M. (2014) Cyclin B2 and p53 control proper timing of centrosome separation. *Nat. Cell Biol.* **16,** 538–549
38. Donzelli, M., and Draetta, G. F. (2003) Regulating mammalian checkpoints through Cdc25 inactivation. *EMBO Rep.* **4,** 671–677
39. Lu, X., Zhu, X., Li, Y., Liu, M., Yu, B., Wang, Y., Rao, M., Yang, H., Zhou, K., Wang, Y., Chen, Y., Chen, M., Zhuang, S., Chen, L. F., Liu, R., and Chen, R. (2016) Multiple P-TEFbs cooperatively regulate the release of promoter-proximally paused RNA polymerase II. *Nucleic Acids Res.* **44,** 6853–6867
40. Peterson, M. G., Inostroza, J., Maxon, M. E., Flores, O., Admon, A., Reinberg, D., and Tjian, R. (1991) Structure and functional properties of human general transcription factor IIE. *Nature* **354,** 369–373
41. Luo, Z., Lin, C., Guest, E., Garrett, A. S., Mohaghegh, N., Swanson, S., Marshall, S., Florens, L., Washburn, M. P., and Shilatifard, A. (2012) The super elongation complex family of RNA polymerase II elongation factors: Gene target specificity and transcriptional output. *Mol. Cell. Biol.* **32,** 2608–2617
42. Price, D. H. (2000) P-TEFb, a cyclin-dependent kinase controlling elongation by RNA polymerase II. *Mol. Cell. Biol.* **20,** 2629–2634
43. Orphanides, G., LeRoy, G., Chang, C. H., Luse, D. S., and Reinberg, D. (1998) FACT, a factor that facilitates transcript elongation through nucleosomes. *Cell* **92,** 105–116
44. Mason, P. B., and Struhl, K. (2003) The FACT complex travels with elongating RNA polymerase II and is important for the fidelity of transcriptional initiation *in vivo*. *Mol. Cell. Biol.* **23,** 8323–8333
45. Safina, A., Garcia, H., Commane, M., Guryanova, O., Degan, S., Kolesnikova, K., and Gurova, K. V. (2013) Complex mutual regulation of facilitates chromatin transcription (FACT) subunits on both mRNA and protein levels in human cells. *Cell Cycle* **12,** 2423–2434
46. Subramanian, A., Tamayo, P., Mootha, V. K., Mukherjee, S., Ebert, B. L., Gillette, M. A., Paulovich, A., Pomeroy, S. L., Golub, T. R., Lander, E. S., and Mesirov, J. P. (2005) Gene set enrichment analysis: a knowledge-based approach for interpreting genome-wide expression profiles. *Proc. Natl. Acad. Sci. U.S.A.* **102,** 15545–15550
47. Attwooll, C., Lazzerini Denchi, E., and Helin, K. (2004) The E2F family: specific functions and overlapping interests. *EMBO J.* **23,** 4709–4716
48. Pützer, B. M., and Engelmann, D. (2013) E2F1 apoptosis counterattacked: Evil strikes back. *Trends Mol. Med.* **19,** 89–98
49. Hallstrom, T. C., Mori, S., and Nevins, J. R. (2008) An E2F1-dependent gene expression program that determines the balance between proliferation and cell death. *Cancer Cell* **13,** 11–22
50. Wu, M., Seto, E., and Zhang, J. (2015) E2F1 enhances glycolysis through suppressing Sirt6 transcription in cancer cells. *Oncotarget* **6,** 11252–11263
51. Poppy Roworth, A., Ghari, F., and La Thangue, N. B. (2015) To live or let die: Complexity within the E2F1 pathway. *Mol. Cell. Oncol.* **2,** e970480
52. Jiang, W., Guo, X., and Bhavanandan, V. P. (1998) Four distinct regions in the auxiliary domain of heterogeneous nuclear ribonucleoprotein C-related proteins. *Biochim. Biophys. Acta* **1399,** 229–233
53. Busch, A., and Hertel, K. J. (2012) Evolution of SR protein and hnRNP splicing regulatory factors. *Wiley Interdiscip. Rev. RNA* **3,** 1–12
54. Lemieux, B., Blanchette, M., Monette, A., Mouland, A. J., Wellinger, R. J., and Chabot, B. (2015) A function for the hnRNP A1/A2 proteins in transcription elongation. *PLoS ONE* **10,** e0126654
55. Kang, M. J., Abdelmohsen, K., Hutchison, E. R., Mitchell, S. J., Grammatikakis, I., Guo, R., Noh, J. H., Martindale, J. L., Yang, X., Lee, E. K., Faghihi, M. A., Wahlestedt, C., Troncoso, J. C., Pletnikova, O., Perrone-Bizzozero, N., *et al.* (2014) HuD regulates coding and noncoding RNA to induce APP→Aβ processing. *Cell Rep.* **7,** 1401–1409
56. Dowling, C. M., Herranz Ors, C., and Kiely, P. A. (2014) Using real-time impedance-based assays to monitor the effects of fibroblast-derived media on the adhesion, proliferation, migration and invasion of colon cancer cells. *Biosci. Rep.* **34,** e00126
57. Dickhuth, J., Koerdt, S., Kriegebaum, U., Linz, C., Müller-Richter, U. D., Ristow, O., Kübler, A. C., and Reuther, T. (2015) *In vitro* study on proliferation kinetics of oral mucosal keratinocytes. *Oral Surg. Oral Med. Oral Pathol. Oral Radiol.* **120,** 429–435
58. Massey, A. J. (2015) Multiparametric cell cycle analysis using the Operetta high-content imager and Harmony software with PhenoLOGIC. *PLoS ONE* **10,** e0134306
59. Jao, C. Y., and Salic, A. (2008) Exploring RNA transcription and turnover *in vivo* by using click chemistry. *Proc. Natl. Acad. Sci. U.S.A.* **105,** 15779–15784
60. Singh, J., and Padgett, R. A. (2009) Rates of *in situ* transcription and splicing in large human genes. *Nat. Struct. Mol. Biol.* **16,** 1128–1133
61. Henikoff, S., Henikoff, J. G., Sakai, A., Loeb, G. B., and Ahmad, K. (2009) Genome-wide profiling of salt fractions maps physical properties of chromatin. *Genome Res.* **19,** 460–469
62. Sama, R. R., Ward, C. L., and Bosco, D. A. (2014) Functions of FUS/TLS from DNA repair to stress response: Implications for ALS. *ASN Neuro* **6,** 1759091414544472
63. Yu, Y., and Reed, R. (2015) FUS functions in coupling transcription to splicing by mediating an interaction between RNAP II and U1 snRNP. *Proc. Natl. Acad. Sci. U.S.A.* **112,** 8608–8613
64. Calvio, C., Neubauer, G., Mann, M., and Lamond, A. I. (1995) Identification of hnRNP P2 as TLS/FUS using electrospray mass spectrometry. *RNA* **1,** 724–733
65. Yasuda, K., Zhang, H., Loiselle, D., Haystead, T., Macara, I. G., and Mili, S. (2013) The RNA-binding protein Fus directs translation of localized mRNAs in APC-RNP granules. *J. Cell Biol.* **203,** 737–746
66. Masuda, A., Takeda, J., Okuno, T., Okamoto, T., Ohkawara, B., Ito, M., Ishigaki, S., Sobue, G., and Ohno, K. (2015) Position-specific binding of FUS to nascent RNA regulates mRNA length. *Genes Dev.* **29,** 1045–1057
67. Korotayev, K., and Ginsberg, D. (2008) Many pathways to apoptosis: E2F1 regulates splicing of apoptotic genes. *Cell Death Differ.* **15,** 1813–1814
68. Johnson, D. G. (2000) The paradox of *E2F1*: Oncogene and tumor suppressor gene. *Mol. Carcinog.* **27,** 151–157
69. Müller, H., and Helin, K. (2000) The E2F transcription factors: Key regulators of cell proliferation. *Biochim. Biophys. Acta* **1470,** M1–M12
70. Farra, R., Dapas, B., Pozzato, G., Scaggiante, B., Agostini, F., Zennaro, C., Grassi, M., Rosso, N., Giansante, C., Fiotti, N., and Grassi, G. (2011) Effects of E2F1-cyclin E1-E2 circuit down regulation in hepatocellular carcinoma cells. *Dig. Liver Dis.* **43,** 1006–1014
71. Pellicelli, M., Picard, C., Wang, D., Lavigne, P., and Moreau, A. (2016) E2F1 and TFDP1 regulate PITX1 expression in normal and osteoarthritic articular chondrocytes. *PLoS ONE* **11,** e0165951
72. Ohtani, K., DeGregori, J., and Nevins, J. R. (1995) Regulation of the cyclin E gene by transcription factor E2F1. *Proc. Natl. Acad. Sci. U.S.A.* **92,** 12146–12150
73. Russo, A. J., Magro, P. G., Hu, Z., Li, W. W., Peters, R., Mandola, J., Banerjee, D., and Bertino, J. R. (2006) E2F-1 overexpression in U2OS cells increases cyclin B1 levels and cdc2 kinase activity and sensitizes cells to antimitotic agents. *Cancer Res.* **66,** 7253–7260
74. Vigo, E., Müller, H., Prosperini, E., Hateboer, G., Cartwright, P., Moroni, M. C., and Helin, K. (1999) CDC25A phosphatase is a target of E2F and is required for efficient E2F-induced S phase. *Mol. Cell. Biol.* **19,** 6379–6395
75. Fasken, M. B., Laribee, R. N., and Corbett, A. H. (2015) Nab3 facilitates the function of the TRAMP complex in RNA processing via recruitment of Rrp6 independent of Nrd1. *PLoS Genet.* **11,** e1005044
76. Bondy-Chorney, E., Baldwin, R. M., Didillon, A., Chabot, B., Jasmin, B. J., and Côté, J. (2017) RNA-binding protein RALY promotes protein arginine methyltransferase 1 alternatively spliced isoform v2 relative expression

and metastatic potential in breast cancer cells. *Int. J. Biochem. Cell Biol.* **91,** 124–135

77. Baldwin, R. M., Morettin, A., Paris, G., Goulet, I., and Côté, J. (2012) Alternatively spliced protein arginine methyltransferase 1 isoform PRMT1v2 promotes the survival and invasiveness of breast cancer cells. *Cell Cycle* **11,** 4597–4612
78. Daigle, J. G., Lanson, N. A., Jr., Smith, R. B., Casci, I., Maltare, A., Monaghan, J., Nichols, C. D., Kryndushkin, D., Shewmaker, F., and Pandey, U. B. (2013) RNA-binding ability of FUS regulates neurodegeneration, cytoplasmic mislocalization and incorporation into stress granules associated with FUS carrying ALS-linked mutations. *Hum. Mol. Genet.* **22,** 1193–1205
79. Chen, Y., Zubovic, L., Yang, F., Godin, K., Pavelitz, T., Castellanos, J., Macchi, P., and Varani, G. (2016) Rbfox proteins regulate microRNA biogenesis by sequence-specific binding to their precursors and target downstream Dicer. *Nucleic Acids Res.* **44,** 4381–4395
80. Keene, J. D., Komisarow, J. M., and Friedersdorf, M. B. (2006) RIP-Chip: The isolation and identification of mRNAs, microRNAs and protein components of ribonucleoprotein complexes from cell extracts. *Nat. Protoc.* **1,** 302–307
81. Liberzon, A., Birger, C., Thorvaldsdóttir, H., Ghandi, M., Mesirov, J. P., and Tamayo, P. (2015) The Molecular Signatures Database (MSigDB) hallmark gene set collection. *Cell Syst.* **1,** 417–425
82. Huber, W., Carey, V. J., Gentleman, R., Anders, S., Carlson, M., Carvalho, B. S., Bravo, H. C., Davis, S., Gatto, L., Girke, T., Gottardo, R., Hahne, F., Hansen, K. D., Irizarry, R. A., Lawrence, M., *et al.* (2015) Orchestrating high-throughput genomic analysis with Bioconductor. *Nat. Methods* **12,** 115–121

The hnRNP RALY regulates transcription and cell proliferation by modulating the expression of specific factors including the proliferation marker E2F1

Nicola Cornella, Toma Tebaldi, Lisa Gasperini, Jarnail Singh, Richard A. Padgett, Annalisa Rossi and Paolo Macchi

J. Biol. Chem. 2017, 292:19674-19692.
doi: 10.1074/jbc.M117.795591 originally published online September 27, 2017

The hnRNP RALY regulates transcription and cell proliferation by modulating the expression of specific factors, including the proliferation-marker E2F1

Nicola Cornella[1], Toma Tebaldi[2], Lisa Gasperini[1], Jarnail Singh [4], Richard A. Padgett[3], Annalisa Rossi[1], Paolo Macchi[1]

From the [1]Laboratory of Molecular and Cellular Neurobiology, Centre for Integrative Biology, University of Trento, via Sommarive 9, 38123, Trento, ITALY.
[2]Laboratory of Translational Genomics, Centre for Integrative Biology, University of Trento, via Sommarive 9, 38123, Trento, ITALY.
[3]Lerner Research Institute, 9500 Euclid Avenue, Cleveland, Ohio 44195, USA.
[4]Deciphera Pharmaceuticals, 643 Massachusetts St 200, Lawrence, KS 66044, USA.

Running title: *RALY regulates RNA transcription and E2F1 expression*

To whom correspondence should be addressed: Annalisa Rossi (annalisa.rossi-1@unitn.it), Paolo Macchi (paolo.macchi@unitn.it), Tel: +39-0461-283819; Fax: +39-0461-283937

Keywords: RNA, RNA metabolism, heterogeneous nuclear ribonucleoprotein (hnRNP), hnRNP-associated with lethal yellow homolog (RALY), chromatin, transcription, E2F transcription factor

---

SUPPLEMENTARY MATERIAL

FIGURES

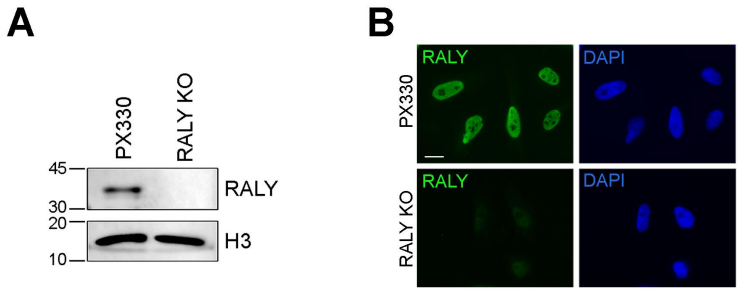

Supplementary Figure S1. RALY KO cells do not express RALY. (**A-B**) Stable RALY knockout HeLa cells (RALY KO) and control cells (PX330) were analysed both by SDS/PAGE and Western blot (**A**) and by immunofluorescence analyses (**B**) to assess RALY expression. In both the cases, RALY was not detected in RALY KO cells. Scale bar = 10 μm.

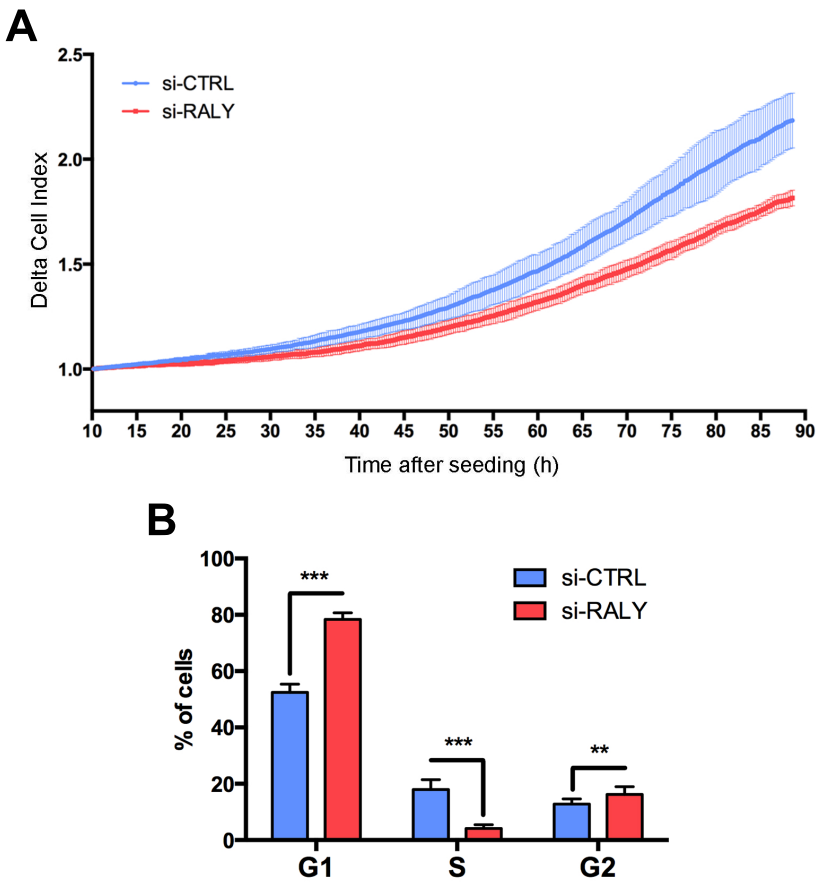

Supplementary Figure S2. The silencing of RALY impairs cell proliferation and cell cycle progression. (**A**) HeLa cells were transfected for 72 hours either with si-CTRL or si-RALY and then plated into an xCELLigence RTCA E-plate. Cell proliferation was monitored for 90 hours. Si-RALY cells show a decreased cell proliferation compared to si-CTRL cells. (**B**) HeLa cells were transfected for 72 hours either with si-CTRL or si-RALY and then seeded into a 96-well plate and left to grow for 24 hours. The cells were then incubated with 10 μM 5-EdU for 1 hour and processed to stain newly synthesized DNA. The cells were analysed by the High Content Imaging System and the distribution of the cells through the cell cycle was evaluated depending on their DNA content. Si-RALY cells show an enrichment in the G1 phase of the cell cycle and a lower presence in S phase compared to si-CTRL cells. There is a significant higher abundance of si-RALY cells in G2 phase, but it only consists in a 4% increase compared to si-CTRL cells. The graph shows the mean values of three independent experiments. Bars represent mean ± S.D. P-value was calculated by unpaired two-tailed t-test (**P<0.01; ***P < 0.001).

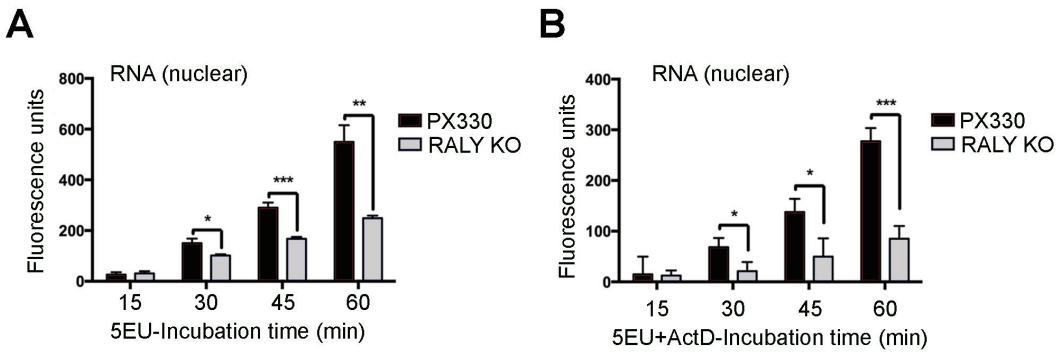

Supplementary Figure S3. RALY knock-out HeLa cells show a decreased RNAPII-dependent transcription. (**A-B**) RALY KO and PX330 cells were incubated with 5EU (**A**) or with 5EU plus ActD (125 ng/ml) (**B**) for 0, 15, 30, 45 and 60 minutes to measure RNA synthesis. The amount of newly synthesized RNA was measured after the staining of the incorporated 5EU with 5-FAM by the high-throughput fluorescence microscope. In both the ActD treated and untreated conditions, the levels of newly synthesized RNA showed a slower increase over time in RALY KO cells compared to PX330 cells, suggesting that the absence of RALY impairs RNA Polymerase II-dependent transcription. The graphs represent the mean of three independent experiments ± S.D. P-value was calculated using an unpaired two tailed t-test between the respective samples (*P<0.05; **P<0.01; ***P<0.001).

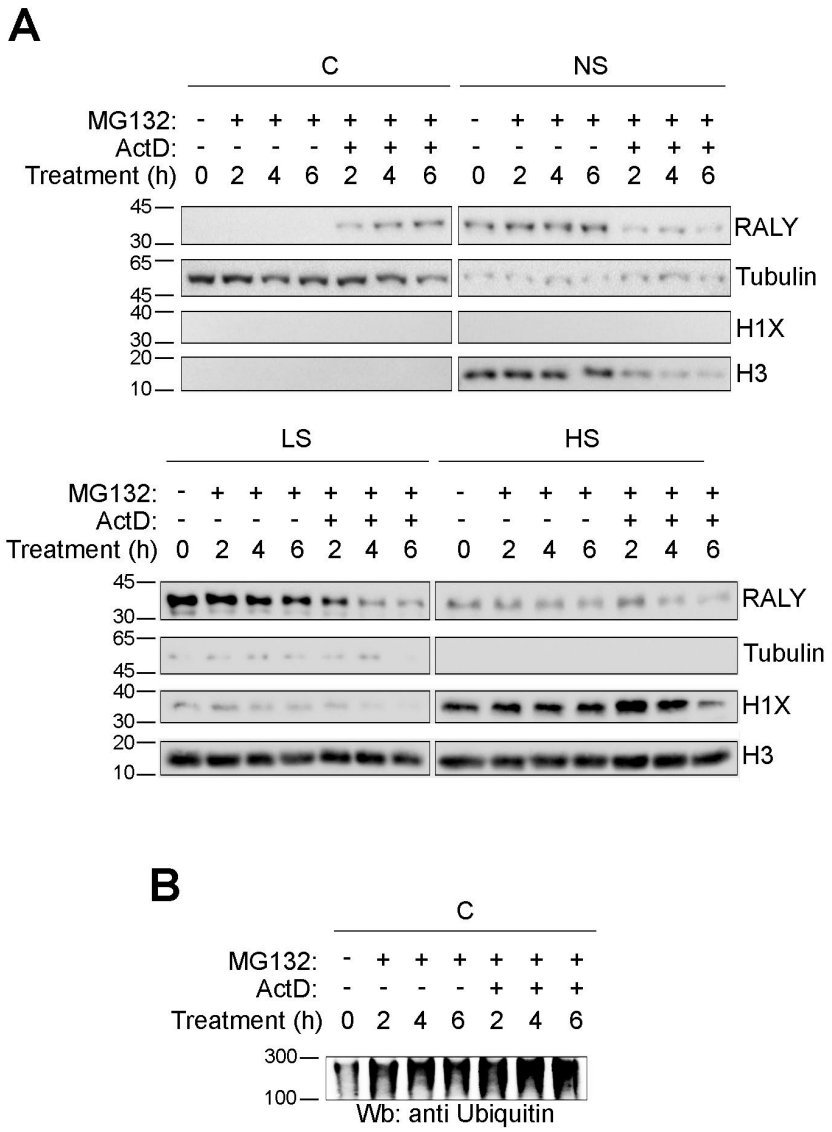

Supplementary Figure S4. RALY is not degraded by the proteasome. (**A-B**) HeLa cells were treated with ActD (5 μg/ml) either with or without 5 mM of the proteasome inhibitor MG132 for 0, 2, 4 or 6 hours. At each time point, the cells were fractionated into cytosolic (C), nuclear-soluble (NS), low-salt soluble chromatin (LS) and high-salt soluble chromatin (HS) fractions. Then, each fraction was subjected to SDS/PAGE and Western blot with the indicated antibodies. (**A**) RALY progressively decreased in the LS fraction and in parallel increased in the C fraction only when the cells were treated with ActD, regardless of the MG132 treatment. Upon transcription block, RALY shifts from the LS to the C fraction and is not degraded from the LS fraction and synthesized *de novo* to remain in the cytoplasm. (**B**) The effectiveness of the MG132 treatment was confirmed through Western blot by the progressive accumulation of Ubiquitin in the C fraction, both in the absence and in presence of ActD.